A LABORATORY INVESTIGATION INTO THE ORIGINS OF METEORITIC ORGANICS BY AQUEOUS ALTERATION OF POLYCYCLIC AROMATIC HYDROCARBONS

by

ERIK SAPERSTEIN

A THESIS

Submitted to the graduate faculty of The University of Alabama at Birmingham,
in partial fulfillment of the requirements for the degree of
Master of Science

BIRMINGHAM, ALABAMA

2005

ABSTRACT OF THESIS
GRADUATE SCHOOL, UNIVERSITY OF ALABAMA AT BIRMINGHAM

Degree M.S. Program Physics

Name of Candidate Erik Saperstein

Committee Chair Perry Gerakines

Title A Laboratory Investigation Into the Origins of Meteoritic Organics by Aqueous Alteration of Polycyclic Aromatic Hydrocarbons

There is strong evidence that meteorite parent bodies have been altered by the action of liquid water. The presence of carbonates suggests that CO_2 was dissolved in the aqueous fluid, and the probable occurrence of NH_3 can be inferred from the spectra of comets and icy satallites. Carbonaceous chondrites also contain organic carbon, mostly bound in an aromatic macromolecule, but a small amount is free, including aromatic and aliphatic hydrocarbons and a suite of biologically important molecules. The free aromatics may have resulted from aqueous alteration of the macromolecule, and it has been suggested that aqueous alteration of the free aromatics may have produced some of the biologically important molecules.

We examined the latter possibility by sealing pyrene and water in a microreactor with 1 bar NH_3 and 25 bar CO_2 for as long as 20 days. Solid products were analyzed by Fourier transform infrared spectroscopy (FTIR). Water soluble products included copious amounts of ammonium carbonate and a small amount of urea. An olive green insoluble fraction was also produced. The principal component of this fraction was siderite, a corrosion product of the stainless steel reaction vessel. The identification of siderite was confirmed by ^{57}Fe Mössbauer spectroscopy. The remainder of the insoluble fraction seemed to be an aromatic nitrogen heterocycle. This aromatic component is probably partially hydrogenated, with amine and hydroxyl groups. An experiment in which olivine was included with the pyrene yielded a different insoluble organic material, probably a hydrogenated and hydroxylated aromatic compound, but no siderite.

TABLE OF CONTENTS

Page

TABLE OF CONTENTS (CONTINUED)

Page

LIST OF TABLES

LIST OF FIGURES

LIST OF FIGURES (CONTINUED)

LIST OF FIGURES (CONTINUED)

1. INTRODUCTION

About 5% of all meteorite falls on Earth comprise the class of meteorites known as carbonaceous chondrites. Like ordinary chondrites, they consist of aggregations of glassy mineral inclusions, called chondrules; however, in this case the chondrules are embedded in a dark, black carbonaceous matrix. These meteorites have bulk elemental abundances very similar to those of the Sun, indicating that they have remained essentially unaltered since their formation in the Solar nebula. In fact, this match is so good that Solar abundances for elements whose values are too low to determine spectroscopically are determined by their values observed in chondrites (Anders & Grevesse, 1989; Burnett et al., 1989). Another source of such primitive materials is micrometeorites in the form of interplanetary dust particles. The composition and structure of most interplanetary dust particles are very similar to that of carbonaceous chondrites. Interplanetary dust particles represent a continuous, and continuing, source of extraterrestrial materials to Earth, with a flux that makes the mass contribution of carbon from meteorites practically negligible (Anders & Grevesse, 1989). Nonetheless, only meteorites can yield information about processes that occurred during planetesimal formation; and, although their bulk compositions are very similar, the specific organization of their materials varies.

As their name implies, carbonaceous chondrites contain a significant amount of carbon, although it represents only about 5% of the meteorite's total mass (Sears, 1978). The primary significance of this carbon lies in its organization into a variety of free organic molecules, including amino acids (Cronin & Moore, 1971), sugars (Cooper et al., 2001), nucleic acids (Stoks & Schwartz, 1981), fatty acids, and light aromatic compounds, as well as a macromolecular material containing polycyclic aromatic hydrocarbon (PAH) structures (Hayatsu et al., 1977). The nature of the organic content of these meteorites spans the full range of the most basic materials involved in the living systems on Earth and may provide a link between life on Earth and the pre-biotic chemistry in the early Solar System. Moreover, PAHs seem to be a significant repository of carbon in the interstellar medium (Allamandola et al., 1985), thus extending this link from the pre-Solar nebula to interstellar materials, and the stars that originally produced them.

The connection between the organics in carbonaceous chondrites and the pre-biotic chemistry of the Solar nebula is the carbon content of these meteorites, and in particular, the possible association between the free organic material and the macromolecular material. The link between these materials remains poorly understood, but there is some indirect evidence that they may be related. Sephton et al. (1998) have shown that the labile portion of the macromolecular material extracted from the Murchison carbonaceous chondrite is sufficiently enriched in ^{13}C relative to the free aromatic hydrocarbons so as to suggest that the material could have been produced by a preterrestrial degradation event, such as hydrous pyrolysis. However, Sephton et al. (1998) have also suggested that this macromolecular material is not enriched enough to have produced certain other constituents of the free organic material, such as light alkyl hydrocarbons, carboxylic acids, and amino acids. Other sources of carbon are needed to produce the ^{13}C enrichments observed in these compounds. This does not mean that the macromolecular material could not have participated in the formation of these molecules, but it does imply that it can not have been the sole parent.

The fact that this macromolecular kerogen-like material is indeed interstellar in origin, as is required to complete the star-meteorite connection, is evidenced by the D/H ratios of these materials. The results of Kerridge et al. (1987) imply a

D enrichment of up to 1,800 per mil, relative to terrestrial standards, for samples of this material from Murchison, suggesting that this material is at least partially interstellar in origin. Yang & Epstein (1983) have measured the D/H ratios of organic matter in a variety of meteorites, including non-carbonaceous chondrites, and in all instances have found D enrichments, relative to terrestrial standards, that are comparable to those observed by Penzias (1980) and Wannier (1980) for HCN and HCO^+ in interstellar clouds in our galaxy.

Despite the fact that these meteorites are extremely heterogeneous in composition, there is evidence for alteration of their materials while they were still incorporated in their parent bodies. Stony-iron and iron meteorites present clear evidence of strong thermal alteration, while many chondrites show features consistent with aqueous alteration of their primary mineral phases. Veins of water-soluble salts, precipitated iron minerals, and hydrated silicates (Wdowiak & Agresti, 1984; Buseck & Hua, 1993) suggest that liquid water once interacted with mineral assemblages in carbonaceous chondrites. Suggested sources of this water include accreted ice (Grimm & McSween, 1989) and hydrated mineral phases. The heat required to melt this ice or release adsorbed water may have come from the radioactive decay of ^{26}Al in the meteorite parent body. Gases released during melting and aqueous alteration could have become encapsulated within the parent body, leading to pressurized pockets of material (Wilson et al., 1999). Under conditions of elevated temperature and pressure, water can become near-critical. The critical point of water is 373°C and 218 bar. Near its critical point, the equilibrium state of water shifts toward H^+ and OH^-, and it therefore becomes very reactive.

When acting on organic matter, supercritical water behaves very much like an organic acid (Katritzky et al., 2001). In particular, this hydrous pyrolysis of kerogen-like material tends to result in depolymerization and the production of less-substituted PAHs (Katritzky et al., 2001). Pure PAHs tend to remain unreactive in supercritical water, producing primarily hydrated species. On the other hand the addition of a second carbon phase, such as CO_2 or CO released from a reaction between water and a source of carbon, produces some methyl- and ethyl-substituted PAHs, whereas the release of H_2 leads to increased hydrogenation (McCollom et al., 1999). Studies of isotopic exchange between PAHs and near-critical D_2O show that their aromatic parts become completely deuterated, whereas alkyl-substituted parts may or may not become deuterated, depending on the reaction conditions (Junk & Catallo, 1996).

If such conditions were met within the meteorite parent bodies, their organic content – including the macromolecular material – should have been aqueously altered along with the minerals. Shock & Schulte (1990) suggest that aqueous alteration of PAHs with CO_2 and NH_3 could have produced some of the organics observed in meteorites, including amino acids and carboxylic acids. They further suggest that the excesses of ^{13}C in CO_2 and ^{15}N from low-temperature methanol extracts from Murchison could have mixed with the depleted ^{13}C and ^{15}N in the macromolecular material to produce the observed enrichments of these isotopic ratios in amino acids and carboxylic acids observed in this meteorite. This is also consistent with the observed association of phyllosilicate mineral clays and organic matter in the Murchison, Ivuna, Orgueil, and Tagish Lake carbonaceous chondrites (Pearson et al., 2002).

The suggestion by Shock & Schulte (1990) that the aqueous alteration of PAHs may have produced some of the organics produced in meteorites led us to investigate this possibility through a series of laboratory experiments. In these laboratory experiments, the PAH pyrene was sealed in a micro-reactor with H_2O, CO_2, and NH_3 at 100°C near 30 bar for as long as 20 days. Shock & Schulte (1990) also suggested that some of the minerals in meteorites were altered in the same aqueous alteration event as the organics, and that the two may have been linked. The primary minerals in the matricies of carbonaceous chondrite meteorites are olivine and phyllosilicates (Buseck & Hua, 1993). Olivine converts to the phyllosilicate mineral serpentine under hydrothermal conditions. Therfore, in one of these experiments, the mineral olivine was included in the reactor to test the interdependence of the organic reactions with the mineral reactions.

Chapter 2 describes the experimental equipment, parameters, and methods. The results are presented in Chapter 3. Chapter 4 contains a discussion of the results and suggestions for the future direction of this research.

2. EXPERIMENTAL METHODS

2.1 Equipment

In the laboratory, a high pressure micro-reactor (Parr Instrument Company, #4790) was used to simulate the physical conditions in a primitive asteroidal body (see Figure 1). The reactor is composed of a type 316 stainless steel vessel and head. A pair of collars keeps the head pressed against the vessel, and the pressure seal is made by a Teflon gasket between the head and vessel. The head is equipped with a pressure gauge (with ticks every 5 bar), thermocouple, gas release valve, liquid sampling valve, gas inlet valve, and a rupture disk to protect against overpressurizing the reactor. A heater surrounds the vessel below the head and is controlled through the thermocouple using an auto-tuning temperature controller (Parr Instrument Company, #4835). The auto-tuning feature was used in every experiment and typically stabilized the temperature to within about 1°C of its set value. A 25 ml Teflon liner inside the vessel served as an inert container for the liquids and solids.

2.2 Chemical and Physical Conditions

The environment within the micro-reactor was chosen to correspond roughly with the conditions of the metastable thermodynamic equilibrium calculations performed by Shock & Schulte (1990). Specifically, these calculations predicted the action of H_2O, CO_2, and NH_3 on either pyrene or fluoranthene, which are isomeric PAHs with the molecular formula $C_{16}H_{10}$, at a temperature of 100°C and a pressure of 100 bar.

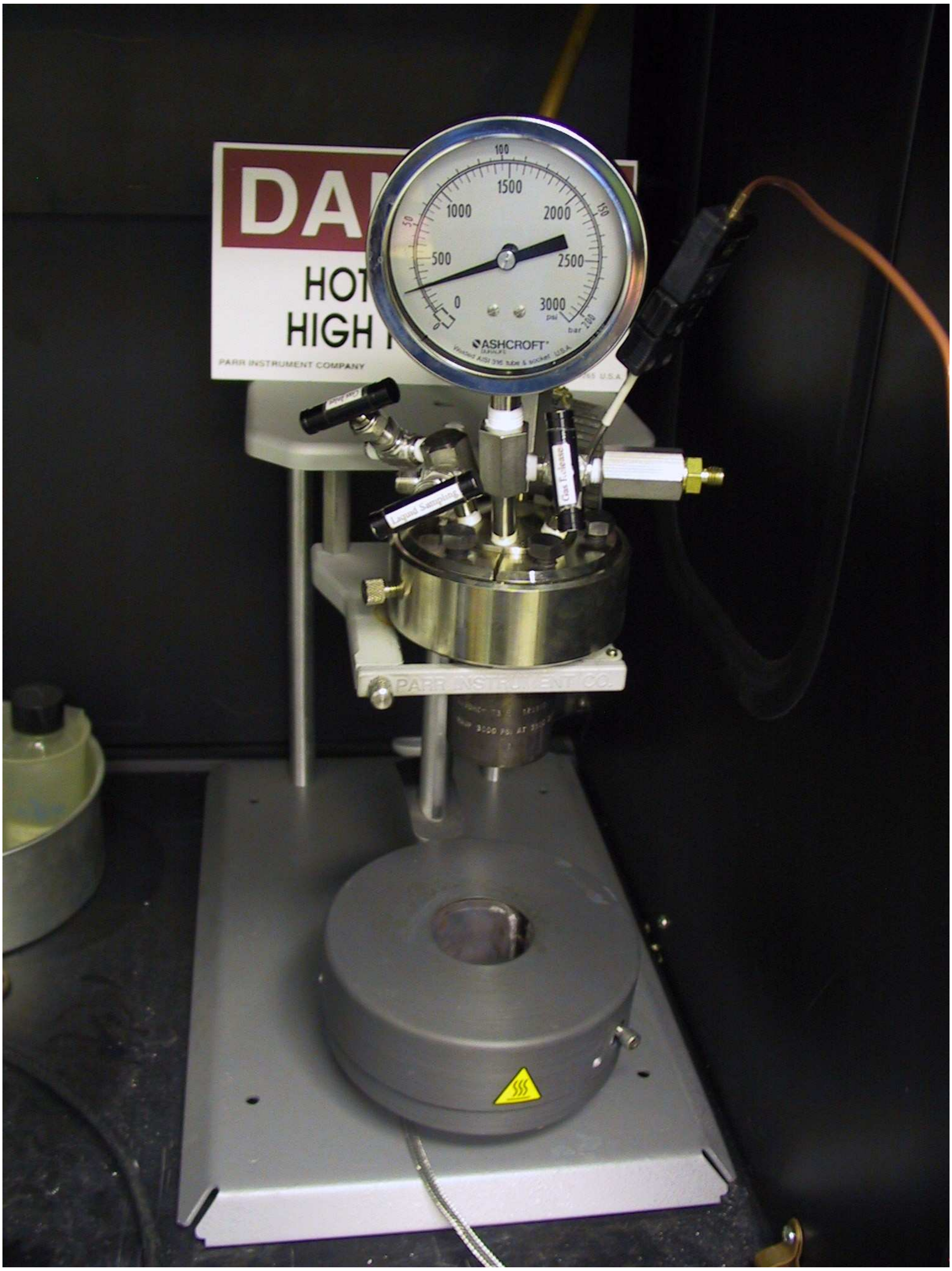

Fig. 1.—The high pressure micro-reactor used in these experiments.

In their calculations with pyrene, Shock & Schulte (1990) set the activity of H_2O at unity, the activity of pyrene at $\log a_{\mathrm{pyrene}} = -2$, the fugacity of CO_2 at $\log f_{\mathrm{CO_2}} = 1.4$, and the fugacity of NH_3 at $\log f_{\mathrm{NH_3}} = -3$. The conditions of our experiments were determined from these values by naively assuming that activity and fugacity could each be equated with partial pressure, i.e. that intermolecular forces could be neglected. This assumption is not fully warranted, since these molecules interact readily, and pyrene is a solid at standard atmospheric pressure and temperature, but it did provide a set of starting conditions.

Because the calculations of Shock & Schulte (1990) explicitly assumed the presence of *liquid* water, 5 ml of water were used in each run to ensure that excess liquid water was present throughout each experiment. The vapor pressure of water at 100°C is 1 bar, and this was used to set the scale of the unitless fugacities quoted above. This resulted in partial pressures of 25 bar of CO_2 and 1 mbar of NH_3. It was difficult to deliver such small pressures of NH_3 to the reactor, so this was increased to 1 bar NH_3. The resulting calculated partial pressure for pyrene was 10 mbar. This was converted into mass by using the ideal gas law, yielding around 2 mg (in 25 ml at 300 K). This amount was too small to work with (the yields were too small), so the initial amount of pyrene was increased to 20 mg.

The total pressure of the CO_2, NH_3, and H_2O at room temperature was 26 bar. At 100°C, this increased to about 32 bar. This is much less than the 100 bar used by Shock & Schulte (1990), and no additional gases were added to bring the pressure up to this value. Presumably, the additional 68 bar would simulate the weight of overlying material at some depth within the meteorite parent body. If this parent body is taken to be an asteroid, it would probably have a diameter of about 200 km. If the density ρ of this asteroid is assumed to be constant throughout its body, then the pressure at some distance r from the center of a body with radius R is given by

$$P = \frac{2\pi}{3} G\rho^2 \left(R^2 - r^2\right) \tag{2.1}$$

(Hartmann, 1993, p.247). The burial depth $d = R - r$ at which a given pressure is reached is therefore given by

$$d = R - \sqrt{R^2 - \frac{3P}{2\pi G\rho^2}}. \tag{2.2}$$

If the body is assumed to have a mean density of 2200 kg/m^3 (similar to carbonaceous chondrites) and a radius of 100 km, then the pressure at the center of the asteroid would approach 68 bar. Carbonaceous chondrites are quite brittle, so one may expect that, even if the entire body were chemically homogeneous, the interior material would be more compact than on the surface (i.e. the density should increase toward the center). If the bulk of the body were assumed to have a mean density of 3500 kg/m^3 (typical of ordinary chondrides, and rocky materials in general), then a pressure of 68 bar will be reached at a depth of about 22 km. However, the large amount of Solar gases retained in C1 carbonaceous chondrites suggests that they originate in a layer of megaregolith only 0.1 km to 0.3 km thick (Heymann 1978), and chondrites in general seem to have been buried beneath about 2 km to 50 km of material (Wasson, 1974, p.185). It does not seem likely that the more primitive carbonaceous chondrites formed under such high pressures. If carbonaceous chondrites were buried beneath about 2 km of material, the pressure of the overlying rock would be about 3 bar to 7 bar, depending on whether the material were carbonaceous or ordinary chondritic in nature, respectively. For these reasons, it was decided to operate at the lower pressure of 32 bar for this first set of experiments.

2.3 Charging the Reactor

Before each experiment, the interior surfaces of the vessel and head, and all surfaces of the sample cup were cleaned using deionized water, acetone, methanol, and deionized water again, in that order. The valves and connecting tubes were also flushed with the same solvents in the same order. Then several milliliters of deionized water were added to the vessel, the head was pressed against it to form a seal, and the reactor was shaken gently upside down for several seconds. This freed particulate material from the valves and connecting tubes. The interior surfaces of the vessel and head, and the valves and connecting tubes were rinsed again using deionized water. The shaking and rinsing continued in this fashion until no more particulate material was evident for three consecutive cycles.

After the first few sets of experiments (for each experiment after S12; see Section 3.1 for list of experiments), the reactor was cleaned further by adding several milliliters of deionized water to the vessel, sealing the reactor, and heating it to 150°C for one day. This freed more particulate material from the valves as well as CO_2 and NH_3 adsorbed to the vessel surfaces. The vessel, head, and valves were then rinsed with deionized water again and the unit shaken again, as above. This series of heating, rinsing and shaking was repeated two more times, but in the last heating, the deionized water was added to the sample cup, instead of directly to the vessel, and the cup inserted into the vessel. After the vessel had been cleaned, it was charged with fresh reactants for the next experiment.

At the start of each experiment, the appropriate solid was weighed using a Mettler H10 analytical balance, accurate to 0.1 mg. Solids used in these experiments were pyrene (Aldrich, 99+%), naphthalene (“Aer-O-Matic” moth flakes), ammonium carbonate (Fisher Scientific, A652-3), and olivine (Ward’s study pack). The pyrene was gently crushed in a folded sheet of weighing paper with the flat end of a metal spatula. The olivine was prepared by removing a piece from the whole rock with a chisel and crushing it in a rock press with a hammer. The resulting gravel was separated by size with a sieve, and the smallest fraction ($<$250 μm in size) retained.

5 ml of water (HPLC Grade, Aldrich) was poured into the sample cup first, followed by solids. The PAHs would typically float, the olivine sank, and the ammonium carbonate dissolved completely. (The pyrene sank while preparing the ammonium carbonate and olivine experiments.) After the water and solids were added, the reactor was sealed and attached to a gas mixing line through the gas sampling valve of the reactor. The gas inlet valve was not used to charge the reactor because it protrudes into the vessel below the water level, precluding the removal of the air in the head space. The mixing line was pumped down to approximately 1 or 2 torr before opening the gas sampling valve to remove the air in the head space of the vessel. The reactor was pumped down to 5 torr before closing the gas sampling valve. A hot air gun was used to evaporate the water that had adsorbed to the interior surfaces of the tubes until the pressure returned to 1 or 2 torr. The mixing line was then pressurized with NH_3 from a lecture bottle (Mathesson, 99+%). The gas sampling valve was then opened until the reactor gauge read about 1 bar. After closing the valve, the reactor pressure immediately fell back to zero as the NH_3 dissolved in the water. The mixing line was pumped out and repressurized with CO_2 (Matheson, 99.8%). The gas sampling valve was reopened until the pressure rose to around 25 bar. After closing the valve, the reactor pressure immediately fell again, usually stablizing between 20 and 25 bar. In some experiments, the steps involving CO_2 and/or NH_3 were omitted, as necessary (see Section 3.1).

2.4 Sample Collection

After removing the reactor from the mixing line, it was immediately set in the heating unit. The heating unit was raised to surround the vessel, the temperature controller was set to maintain the appropriate temperature (typically 100°C), and the unit turned on. Temperature and pressure were noted at the start of the experiment and at intervals throughout the experiment. Generally, the temperature and pressure stabilized after 45 minutes.

After the required duration for the experiment had elapsed, the heater was turned off and the vessel was allowed to cool. Four glass vials with a “press down” lid were cleaned with acetone, methanol, and deionized water, in that order, in preparation for sample collection. After one hour, the temperature had typically fallen to about 60°C and the heater was lowered. After two more hours, the temperature usually dropped to 30°C. The temperature and pressure were then recorded before depressurizing the vessel by opening the liquid sampling valve.

While depressurizing the reactor, several drops of liquid would exit with the gas. This liquid was collected in a vial for later analysis. After depressurizing the reactor, it was removed from the heating unit and opened. Liquid was normally found in three places: under the head (hereafter the “lid”), in the sample cup, and in the vessel (between the vessel and cup). The lid usually dried quite quickly, leaving behind a white solid. This was scraped off gently using a metal spatula and collected on weighing paper. The liquid and any solids present in the cup were collected together in a vial. A metal spatula was used to loosen and guide the solid in order to ensure that as much as possible was transferred and collected along with the liquid. This vial was capped very loosely to allow dissolved gases to escape (when it was capped tightly, the cap would shoot off like a popped cork.) The liquid and any solids present in the vessel were collected in a vial and capped loosely to allow dissolved gases to escape, again using a metal spatula to loosen and guide the solid into the vial along with the liquid.

2.5 Sample Isolation

In order to analyze the insoluble material in the cup, it was first separated from the liquid with which it was collected by pouring the liquid into a separate vial. About 1 ml of deionized water was added to the remaining solid and gently swirled to dissolve any ammonium carbonate or ammonium bicarbonate that was present. This also dissolved any free water-soluble substances. This water was poured into another vial. More deionized water was added, swirled, and poured into this vial. The damp solid was then dried under vacuum (at a pressure of about 10 torr). The vial with the dried solid was then capped tightly and set aside for several hours. If the contents of the vial smelled like ammonia after this time, it was rinsed and dried again until the ammonia smell was gone.

The liquid collected from the cup, now separated from the insoluble material, was dried slowly under vacuum in a bell jar. The outgassing of the liquid under vacuum was minimized by adjusting the pressure in the bell jar. When visible outgassing ceased, the pressure was decreased until it became evident again. Once the pressure was decreased below the vapor pressure of water (around 10 torr), care was taken to prevent the liquid from freezing. This would typically happen at pressures below around 4 torr. When the liquid was evaporated as quickly as possible, several hundred milligrams of ammonium carbonate remained in the vial, as determined by its mid-infrared spectrum (see Section 3.4). In order to determine if any other solids were present in smaller quantities, the liquid from later experiments was dried much more slowly, typically at a pressure of around 30 torr for several days. If, after the water had been evaporated, there was still ammonium carbonate present, another milliliter or so of deionized water was added to the vial and dried under vacuum in the bell jar again. This was repeated until no scent of ammonium carbonate remained.

2.6 Preparation of Samples for Analysis

2.6.1 FTIR Spectroscopy

Fourier-transform infrared (FTIR) spectroscopy was used to characterize the solid products isolated from the experiments. Samples were prepared by dispersing about 1 mg of sample in 150 mg of KBr (Buck Scientific, #5231, spectroscopic grade) using a Beckman RIIC, LTD VM-101 vibromill, and then pressing the mixture into a solid disk inside an aluminum collar (3/4" OD × 5/16" ID × 1/4") using a pair of anvils and an Allied heavy duty hydraulic bottle jack (model no. HJ2). Mid-infrared (mid-IR) spectra were obtained from 4000 cm^{-1} to 400 cm^{-1} (2.5 μm to 25 μm) with a resolution of 4 cm^{-1} using a Mattson Polaris FTIR spectrometer. Spectra were referenced against a "blank" KBr disk prepared in the same way as sample disks, but without sample, and were averages of 256 scans each.

2.6.2 Mössbauer Spectroscopy

^{57}Fe Mössbauer spectroscopy was performed to identify iron-bearing compounds in the insoluble material and in the altered and unaltered olivine. Absorbers were prepared by dispersing around 20 mg of sample in 100 mg melted wax (HealthCo, Item 0628298) at 200°C and then pressing the cooled mixture into a disk between two circular wax paper ends. The absorber was then sealed between two circular white paper labels. Spectra were obtained using the Mössbauer spectroscopy facility at the University of Alabama at Birmingham. The experimental arrangement is described in detail by Wade et al. (1999).

3. RESULTS

3.1 Experiments Performed

The experiments performed were intended to probe three fundamental parameters of the reaction suggested by Shock & Schulte (1990): the evolution of the system over time, the effect of varying the initial solid, and the interdependence of the various variables by eliminating one or more at a time. The standard experiment was defined to be 20 mg pyrene, 5 ml deionized water, 1 bar NH_3, and 25 bar CO_2 at 100°C for 5 days. Individual experiments were considered to be variations of these default parameters.

The first series of experiments in Table 1 was performed to examine the time evolution of the system. Six different experiments comprise this group, with time intervals ranging from 18 hours to 20 days. All other variables remained fixed in this group.

The second series of experiments in Table 1 was performed to examine the effect of varying the initial solid. The first experiment in this series used naphthalene instead of pyrene. Naphthalene is a two-ring PAH with the molecular formula $C_{10}H_8$ that is also found in carbonaceous chondrites, whereas pyrene is a four-ring PAH with the molecular formula $C_{16}H_{10}$. The purpose of this experiment was to see how the choice between two different PAHs affected the results. The second experiment in this series was an attempt to more accurately model the conditions in a meteorite parent body by including the mineral olivine in addition to pyrene. Olivine was probably the principal component of the original chondrite matrix material (Buseck & Hua, 1993). Olivine with a grain size of less than 0.25 mm was used to emulate this matrix material, which has a grain size of less than 5 μm

TABLE 1

A List of Experiments Performed in This Study

Experiment Index	Mass of Solid (mg)		Vol. of Water (ml)	P(NH_3) (bar)	P(CO_2) (bar)	Temp. (°C)	Time (days)
S8	20.0	P	5.0	1	25	100	0.75
S10	20.7	P	5.0	1	25	100	1.5
S3	23.1	P	5.0	2-4	25	100	5
S12	20.3	P	5.0	1	25	100	10
S20	20.5	P	5.2	1-2	25	100	10
S21	21.5	P	5.0	1	25	100	20
S17	22.2	N	5.4	1	25	100	5
S22	23.0	P	5.1	1	25	100	10
	380.3	O					
S15	21.7	P	5.1	0	0	100	5
S7	25.5	P	5.2	0	25	100	5
S11	21.3	P	4.8	1	0	100	5
S9	20.0	P	5.0	1	25	22	5
S13	20.4	P	5.0	0	0	100	5
	1000	A					
S23	none		5.0	1	25	100	20

Notes.—Solids were either pyrene (P), Naphthalene (N), Olivine (O), or Ammonium Carbonate (A), as indicated. The experiments were performed in order of increasing index number, but are here arranged in analagous series.

(Buseck & Hua, 1993). The pyrene was used to represent the entire organic carbon content of a carbonaceous chondrite, which is principally an aromatic macromolecule. The amount of olivine added was chosen to agree with the relative fraction of a carbonaceous chondrite that is mineral versus that which is carbonaceous (up to 5% C by weight; Sears, 1978, p.115): 20 mg of organic carbon would imply a 400 mg meteorite and therefore 380 mg of mineral.

The experiments in the final series in Table 1 are controls. They were used to judge the importance of various factors in the alteration of pyrene. The first three experiments in this series tested the action of the gasses by not adding either NH_3, CO_2, or both. The next experiment, S9, examined the effect of temperature.

Only one experiment was performed, wherein the reactor remained at room temperature (22°C). S13 was intended to test the importance of the form in which NH_3 and CO_2 were added. In this experiment, neither NH_3 nor CO_2 were added as a gas; instead ammonium carbonate ($(NH_4)_2CO_3$) was added, which decomposes into NH_3, CO_2, and H_2O. In these four experiments, no attempt was made to ensure that the pressure in the reactor was the same as in the standard experiment (for example, S3). In the final experiment in this series, no pyrene (or any other solid) was added. Note that this experiment ran for 20 days instead of the usual 5 days. This was done to allow a more direct comparison with S21 in the first series.

3.2 Changes in Pressure

Table 2 lists the temperature and pressure at the start, middle, and end of each experiment. In most cases, there was a net decrease in pressure (measured at room temperature) between the start and end of each experiment. There were three exceptions: S11, S13, and S15. S11 was a control experiment in which no CO_2 was added but was otherwise identical to the standard experiment (c.f. experiment S3). There was no change in pressure at room temperature before and after this experiment. S15 was another control experiment in which neither NH_3 and CO_2 were added but was otherwise identical to the standard experiment. In this experiment, the room temperature pressure rose from 0 bar before the experiment to 1 bar at the conclusion of the experiment. The vapor pressure of water at 100°C is 1 bar, so this change could be explained by saturation of the head space with water vapor.

S13 was used to test the dependance of the results of the standard experiment on the initial state of the CO_2 and NH_3. In this experiment, solid ammonium carbonate was added instead of the gases CO_2 and NH_3 but all other parameters were the same as in the standard experiment. After S13, the pressure increased

TABLE 2

A List of the Temperature and Pressure at the Start, Middle, and End of Each Experiment

Experiment	Initial		During		Final		
Index	T (°C)	P (bar)	T (°C)	P (bar)	T (°C)	P	ΔP (bar)
S8	23	23	100	27	22	17	-6
S10	27	20	100	20	32	14	-6
S3	29	20	100	21	22	14	-6
S12	26	20	102	21	29	15	-5
S20	30	20	100	25	28	15	-5
S21	32	23	100	27	33	18	-5
S17	28	21	100	25	30	16	-5
S22	RT	25	100	30	28	20	-5
S15	29	0	100	1	29	1	1
S7	23	24	100	31	26	22	-2
S11	25	1	100	2	26	1	0
S9	23	22	22	18	22	18	-4
S13	24	1	100	7	31	4	3
S23	28	20	100	27	27	18	-2

Note.—RT denotes room temperature where that measurement was not recorded. In the last column, $\Delta P = P_{final} - P_{initial}$.

from 0 bar to 3 bar. If all of the ammonium carbonate were decomposed at the temperature of this experiment (100°C), 20.8 mmol of NH_3 and 10.4 mmol each of CO_2 and H_2O would be produced. The solubility of NH_3 in water at 100°C and 1 bar is 74 g/L, or 21.8 mmol in 5 ml. The solubility of CO_2 in water at 100°C and 1 bar is 1.96×10^{-4} mol% (Lide, 1993), or 0.05 mmol in 5 ml. All of the NH_3 produced would dissolve in the water and all of the CO_2 would fill the head space of the reactor. The pressure in the reactor, which has about 25 ml of head space, at 100°C would then be 13 bar. The recorded pressure at 100°C was 7 bar. Evidently, only half of the ammonium carbonate decomposed. This presumably represents the equilibrium between the formation and decomposition of ammonium carbonate under these conditions. After the reactor cooled to 31°C, the pressure should have dropped from 7 bar to 6 bar if temperature were the only influencing factor. The recorded pressure was 3 bar. This discrepancy may be explained by the establishment of a new equililibrium in favor of increased formation of ammonium carbonate; the solubility of CO_2 in water is greater at 31°C than at 100°C, so more CO_2 would dissolve in the water and react with the dissolved NH_3 to form more ammonium carbonate.

The remainder of the experiments showed a net decrease in pressure and may be explained by examining experiments S7 and S9, both of which were control experiments. In S7, no NH_3 was added but all other parameters were the same as in the standard experiment. On heating, the pressure rose from 24 bar at 23°C to 31 bar at 100°C. The increase in temperature alone would increase the pressure to 30 bar at 100°C. The solubility of CO_2 in water at 25°C and 25 bar is about 1.3 mol% (3.6 mmol in 5 ml water) and at 100°C and 30 bar is about 0.5 mol% (1.4 mmol in 5 ml water) (Diamond & Akinfiev, 2003). On cooling, the pressure dropped from 31 bar at 100°C to 22 bar at 26°C. The decrease in pressure alone would decrease the pressure to 25 bar and the accompanying increased solubility of CO_2 in water would remove an additional 2.2 mmol (2.2 bar in the 25 ml head space). The final pressure would then be 23 bar. This is close to the recorded pressure of 22 bar.

In S9, the standard experiment remained at room temperature (22°C) instead of being heated to 100°C. Here, the pressure started at 22 bar and dropped to 18 bar. This change occurred within the first 1.5 hours of the experiment. The pressure then remained at 18 bar for the remainder of the experiment. The drop in pressure probably represents the establishment of the equilibrium between production and decomposition of ammonium carbonate in the reactor.

All of the other experiments except S23 showed a similar decrease in pressure of 5 or 6 bar. This is similar to the decrease in pressure of 4 bar observed in

S9. None of the experiments were given the time to reach equilibrium before they began (when the temperature reached 100°C). All of the decrease in pressure in these expereiments was probably due to the establishment of the equilibrium between the production and decomposition of ammonium carbonate after the experiment ended. There was ample time for this equilibrium to be reached because it normally took about 3 hours for the reactor to cool and in S9 it took only 1.5 hours to reach equilibrium. The pressure in these other experiments fell 1 or 2 bar more than in S9, so the equilibrium may have been reached only after more ammonium carbonate had been produced (at the expense of CO_2 in the head space). This may have been caused by increased solubility of CO_2 in the water in the reactor after it had been heated to 100°C. It may also have been caused by an excess of ammonia added to the reactor in these experiments. On the other hand, this difference of 1 or 2 bar is below the resolution of the pressure gauge, so it may reflect measurement error.

None of the changes in pressure in any of the experiments can be attributed to the formation of a product other than ammonium carbonate. For example, 1 bar of NH_3 at 25°C in the 25 ml of head space weighs 17 mg. Conversion of the same amount of CO_2 would weigh 44 mg. This is more than the total mass of product, excluding ammonium carbonate, collected in any of the experiments except S21. Though products were definately formed, changes in pressure due to the incorporation of gases into these products was below the resolution of the equipment.

3.3 Material from the Lid

After each experiment, several mg of a white powder would appear on the inner surface of the reactor lid as it dried. The mid-IR spectrum of this substance from the time evolution series of experiments is shown in Figure 2. The prominent, broad bands, for example from 3600 to 2400 cm^{-1} and from 1700 to 1200 cm^{-1},

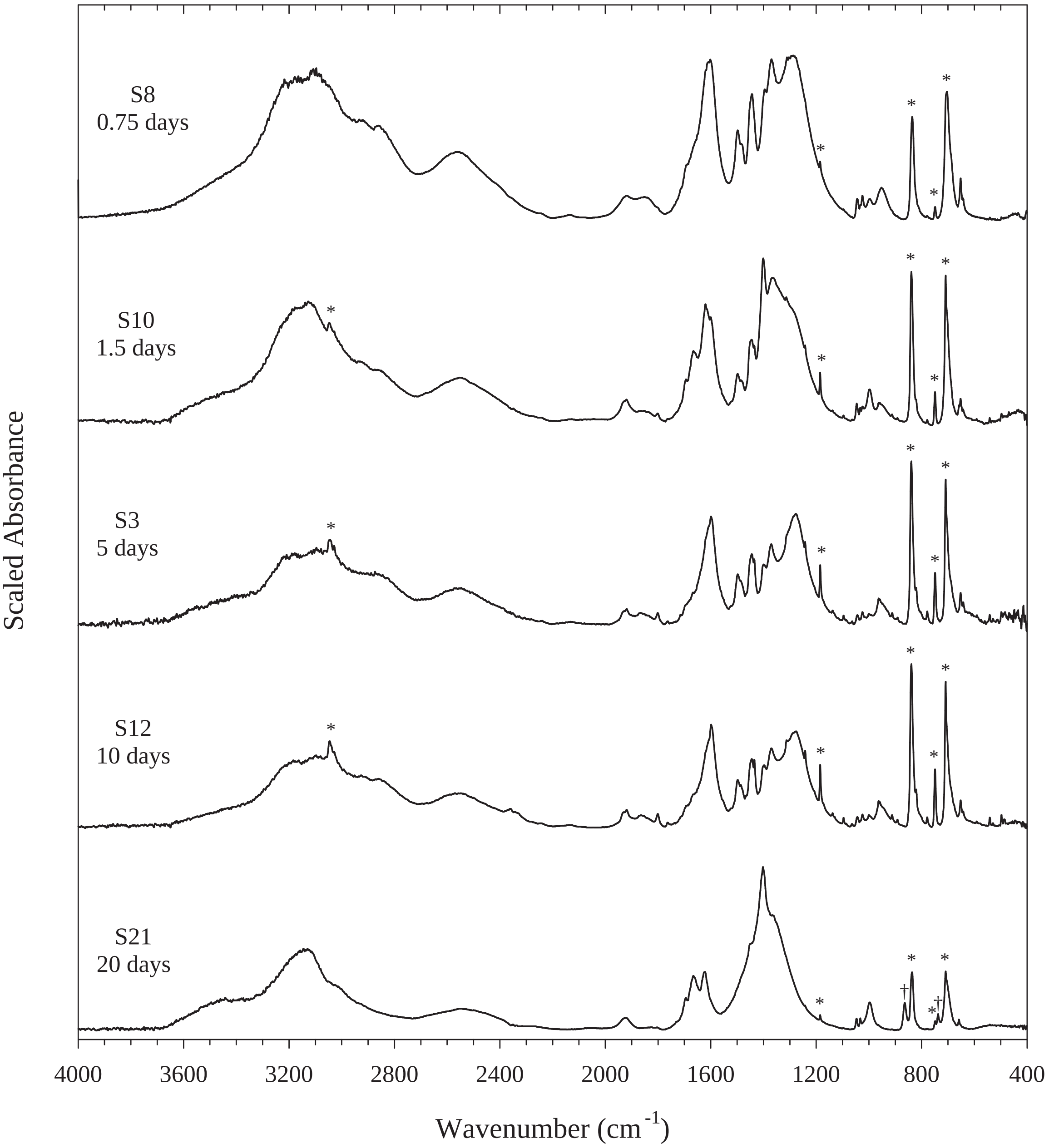

Fig. 2.—Mid-IR spectra of the white powder collected from the lid of the reactor in the time evolution series of experiments. Major peaks of pyrene are marked with asterisks and major peaks of siderite are marked with daggers. Each spectrum has been rescaled to its absorbance at 3145 cm^{-1}.

are due to ammonium carbonate in experiments S8, S3, and S12 and to a mixture of ammonium bicarbonate and ammonium carbonate in experiments S10 and S21. Superimposed on these broad bands are several sharp peaks due to pyrene. These peaks are marked with asterisks in Figure 2. Figure 3 contains a comparison of the spectrum of the material from the lid in experiment S3 with those of ammonium carbonate and pyrene. All peaks in the spectrum of the material from the lid in experiment S3 correspond to those of ammonium carbonate and pyrene, indicating that these are the only materials present in this sample. The general similarity of the spectrum from experiment S3 to the spectra from experiments S8 and S12 indicate that ammonium carbonate and pyrene comprise these samples too. Note that several peaks in the spectrum of the material from the lid in experiment S8, particularly those in the 1700 to 1200 cm^{-1} region, are more blunt or exaggerated relative to corresponding peaks in the spectra from experiments S3 and S12. This was due to excessive sample in that disk, yielding transmission values as low as 1.5% (corresponding to an absorption of 1.8).

Figure 4 contains a comparison of the spectrum of the material from the lid in experiment S10 with those of pyrene, ammonium bicarbonate, and ammonium carbonate. All peaks in the spectrum of the material from the lid in experiment S10 correspond to those of ammonium bicarbonate, ammonium carbonate, and pyrene, indicating that these are the only materials present in this sample. The primary difference between this spectrum and those from S8, S3, and S12 is the dominating presence of ammonium bicarbonate. Close inspection of the spectra of S8, S3, and S12, particularly in the region from 1100 to 900 cm^{-1}, indicate that ammonium bicarbonate is present in these samples as well, though in much smaller amounts. For comparison, a peak at 998 cm^{-1} indicates ammonium bicarbonate, whereas a peak at 953 cm^{-1} indicates ammonium carbonate (cf. Figure 4). This difference in the spectrum from S10 can be explained by the difference between the

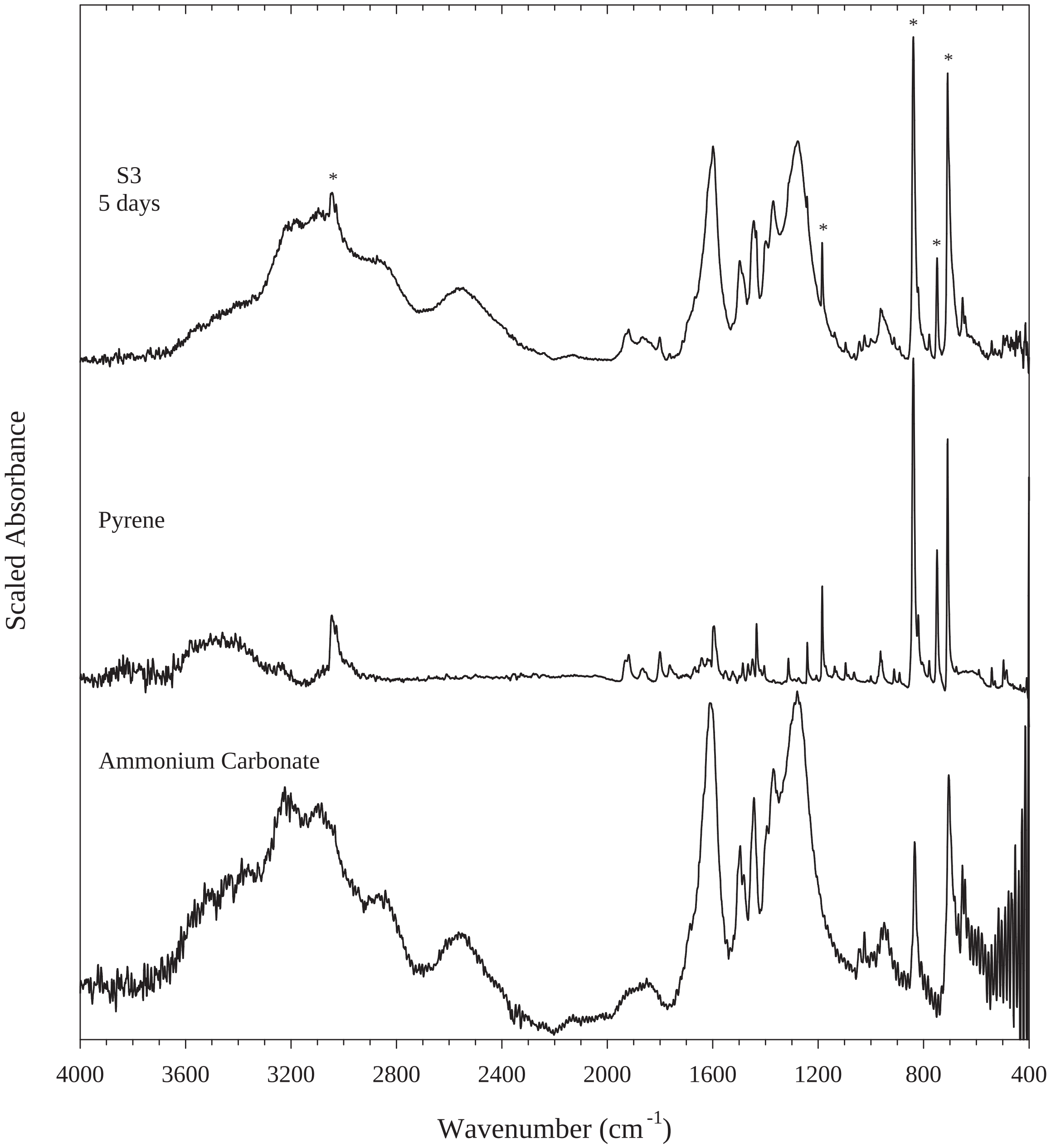

Fig. 3.—Mid-IR spectrum of the white powder collected from the lid of the reactor in experiment S3 (top) compared with the mid-IR spectra of pyrene (middle) and ammonium carbonate (bottom). Major peaks of pyrene visible in the spectrum of S3 are marked with asterisks.

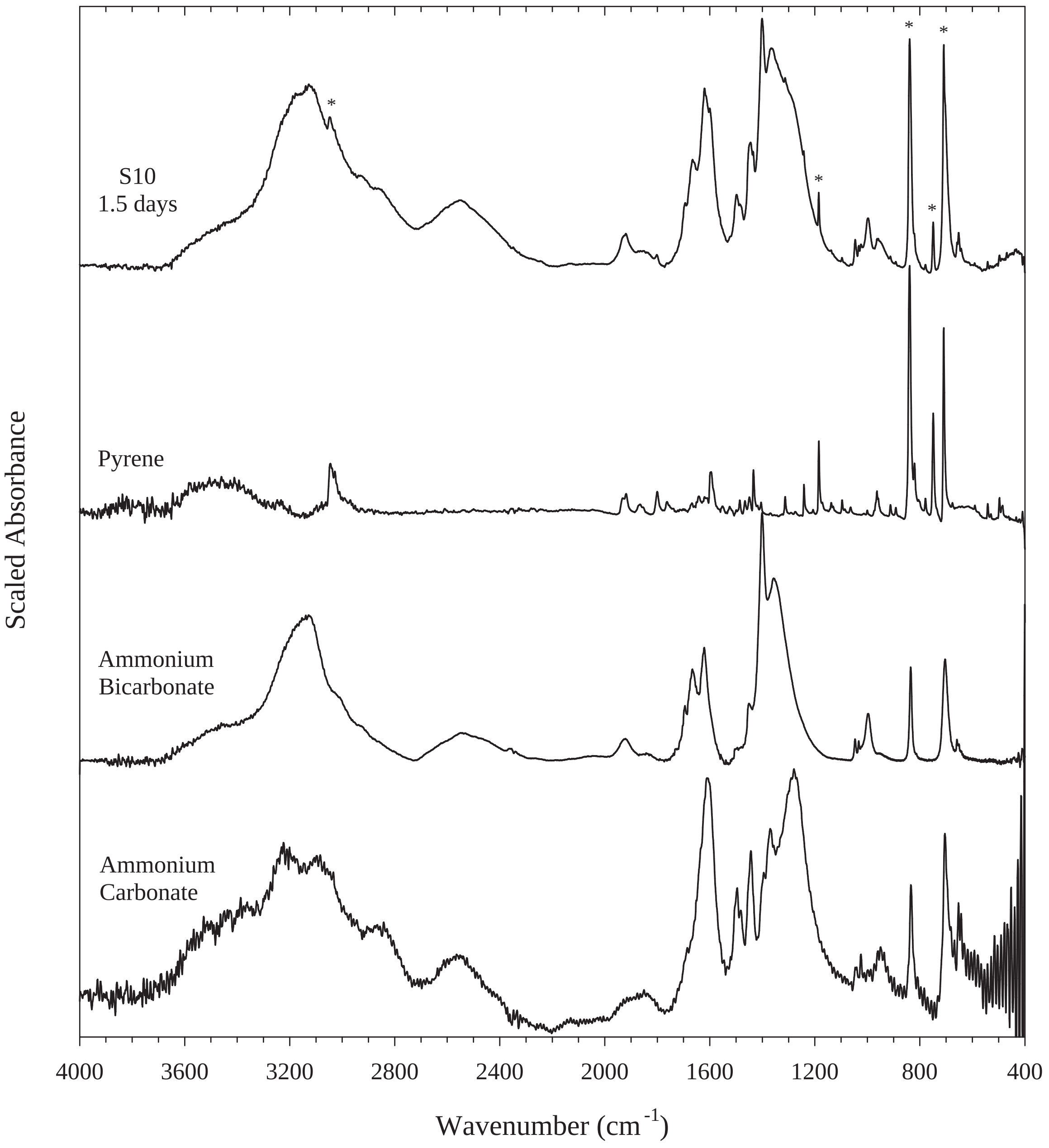

Fig. 4.—Mid-IR spectrum of the white powder collected from the inside lid of the reactor in experiment S10 (top) compared with the mid-IR spectra of pyrene (above-middle), ammonium bicarbonate (below-middle), and ammonium carbonate (botom). Major peaks of pyrene visible in the spectrum of S10 are marked with asterisks.

time the sample was collected and the time the sample was analyzed. Samples from S8, S3, and S12 were analyzed about 1 day after they were collected; that from S10 was analyzed 2 days after collection. In this time, a greater amount of the original ammonium carbonate would have decomposed into ammonium bicarbonate.

Figure 5 contains a comparison of the spectrum of the material from the lid of the reactor in experiment S21 with those of siderite (Ward's study pack; Nova Scotia, Canada) and ammonium bicarbonate. Major peaks due to pyrene in the spectrum from S21 are marked with asterisks. All other peaks are due to ammonium bicarbonate and siderite. Exposed peaks due to siderite are marked with daggers. Unmarked peaks in the spectrum of siderite are due to adsorbed water, not siderite. This is the only sample from the lid that contains siderite. This siderite is a corrosion product of the stainless steel reactor formed by the action of carbonic acid (specifically, CO_2 dissolved in water) on the iron in the stainless steel. Evidently, it only forms in detectable amounts on the lid when the reactor is run for more than 10 days. The absence of ammonium carbonate in this sample is noteworthy, and may be due to the way the sample was stored before collection and analysis.

At the end of experiment S21, the reactor was depressurized but remained sealed until the next day, when the sample was collected. Because the reactor remained sealed, the interior surface of the lid remained wet. Decomposition of aqueous ammonium carbonate into ammonium bicarbonate occurs more rapidly than that of dry ammonium carbonate. Under these conditions, any ammonium carbonate that was originally present may have been converted into ammonium bicarbonate. On the other hand, the absence of ammonium carbonate may indicate a real lack of ammonia in the material from the lid (with an associated incorporation of ammonia elsewhere in the reactor) in this sample relative to the other samples from the lid.

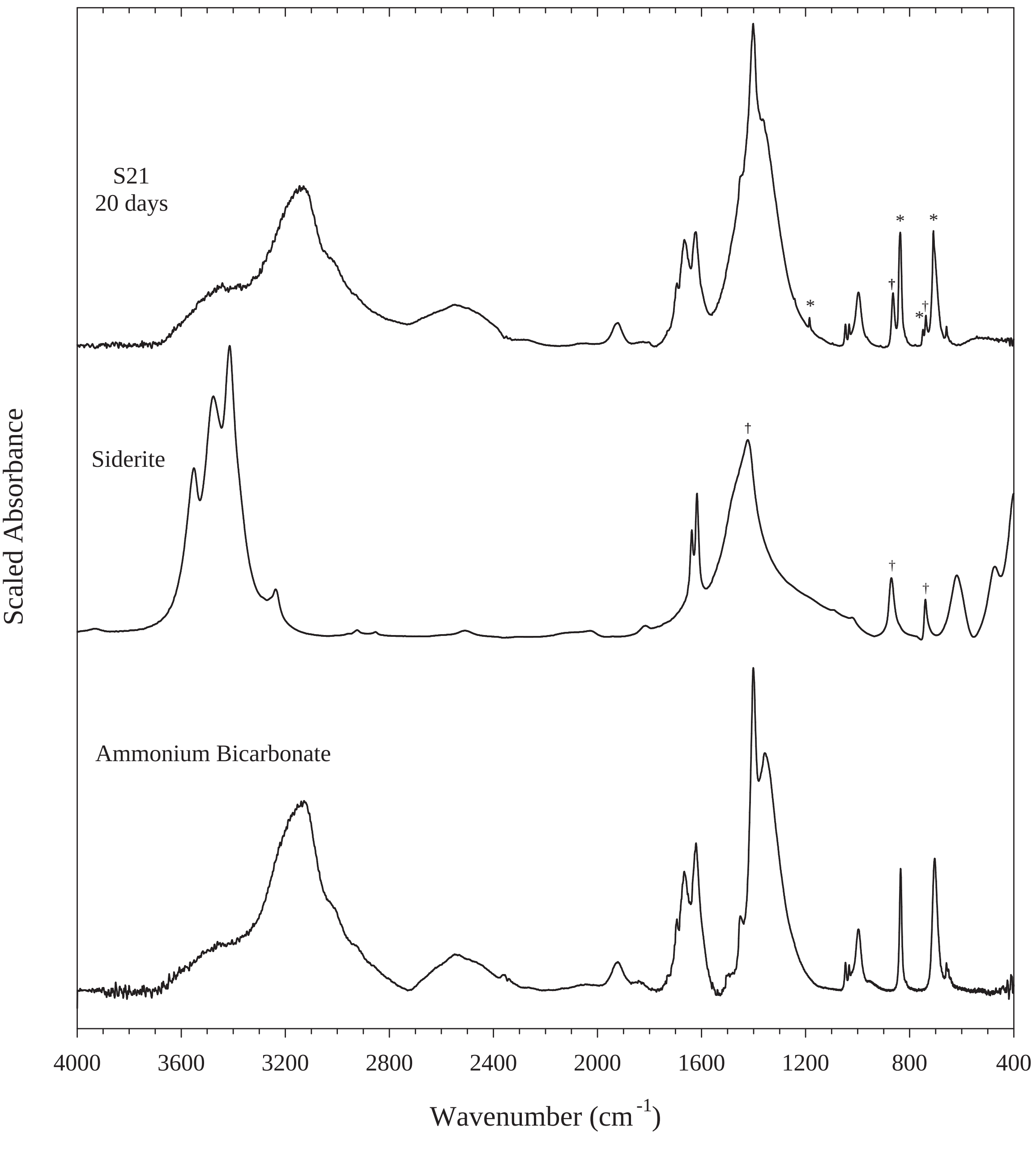

Fig. 5.—Mid-IR spectrum of the white powder collected from the inside lid of the reactor in experiment S21 (top) compared with the mid-IR spectra of siderite (middle) and ammonium bicarbonate (bottom). Major peaks of pyrene are marked with asterisks and exposed peaks of siderite are marked with daggers. Unmarked peaks in the spectrum of siderite are due to water.

The spectra from the second series of experiments were similar to those from the first. The spectrum from S17 revealed a mixture of ammonium carbonate and ammonium bicarbonate, but no naphthelene. After this experiment, the vessel smelled strongly of naphthalene, even after several cleaning cycles. Naphthalene has a high vapor pressure. It is likely that most of the naphthalene condensed in the valves were the temperature was somewhat lower than the vessel, but apparently none condensed on the lid. The spectrum from S22 revealed a mixture of ammonium bicarbonate and pyrene. Ammonium carbonate is absent from this sample for the same reason it was absent in that from experiment S21; the sample remained wet and sealed in the reactor for one day after it was cooled and depressurized.

Of the spectra of the samples from the control experiments, those from S15, S7, S11, and S13 revealed only pyrene, whereas those from S9 and S23 revealed a mixture of ammonium carbonate and ammonium bicarbonate. This is reasonable. S15, S7, and S11 lacked either NH_3, CO_2, or both, so no ammonium carbonate or ammonium bicarbonate could form. All of the ammonium carbonate in experiment S13 was added to the water in the sample cup. None could form on the lid because all of the NH_3 released remained dissolved in the water in the cup. In experiment S9, the vessel was not heated. The pyrene was not volatized and therefore couldn't condense on the lid. In experiment S23, no pyrene was added, so none was found on the lid.

3.4 Soluble Material from the Sample Cup

When the liquid from the cup was dried, hundreds of mg of a white powder would normally remain. The mid-IR spectrum of this material from experiment S3 revealed it to be ammonium carbonate. When the ammonium carbonate was made to decompose by repeatedly wetting and drying the sample, a small amount of white powder would remain. The mid-IR spectra of this material from the first three expreriments of the time evolution series (experiments S8, S10, and S3) are shown in Figure 6, where they are compared with that of urea. The primary features in these spectra are due to urea (NH_2CONH_2). This is clearest in the spectra from S8 and S10. Each major peak in the spectrum of urea corresponds exactly to peaks the spectra of the soluble material from experiments S8 and S10, indicating that urea is present in these samples. The spectrum from experiment S3 is also similar to that of urea, but there are some differences. Both spectra have similar features at the same peak positions, but the strengths and widths of these features are quite different. For example, the spectrum from S3 has a strong, broad feature from 1200 to 900 cm^{-1} that peaks around 1065 cm^{-1}. A similar band is found in the spectra from S8 and S10. The peak of this band in the spectrum from S3 coincides with a minor peak in the spectrum of urea, attributed to the NH_2 antisymmetric rocking mode. This band has a shoulder near 1161 cm^{-1} that corresponds to a peak of moderate intensity in the spectrum of urea, which is due to the NH_2 symmetric rocking mode. Likewise, the spectrum of S3 has broad bands from 1550 to 1350 cm^{-1}, 1650 to 1600 cm^{-1}, and 3600 to 2800 cm^{-1} that roughly coincide with the antisymmetric CN stretching mode (1454 cm^{-1}), the NH_2 bending modes (1638 and 1619 cm^{-1}), CO stretching mode (1664 cm^{-1}), and the NH_2 stretching modes (3442 and 3337 cm^{-1}), respectively, of urea. For reference, the peak postions and vibrational modes of urea in Figure 6 are listed in Table 3 and were inferred from the results of Keuleers et al. (1999). It is possible that all of these features in the spectrum from S3 are due to urea.

In its crystalline state, urea forms an extensive network of hydrogen bonds. This can significantly alter the peak positions and strengths of the vibrational modes of urea. For example, the CO stretching mode of gas phase urea is calculated to occur at 1738 cm^{-1}, whereas in the crystalline state, it occurs at 1601 cm^{-1} (Keuleers et al., 1999). The spectrum of urea in Figure 6 more closely

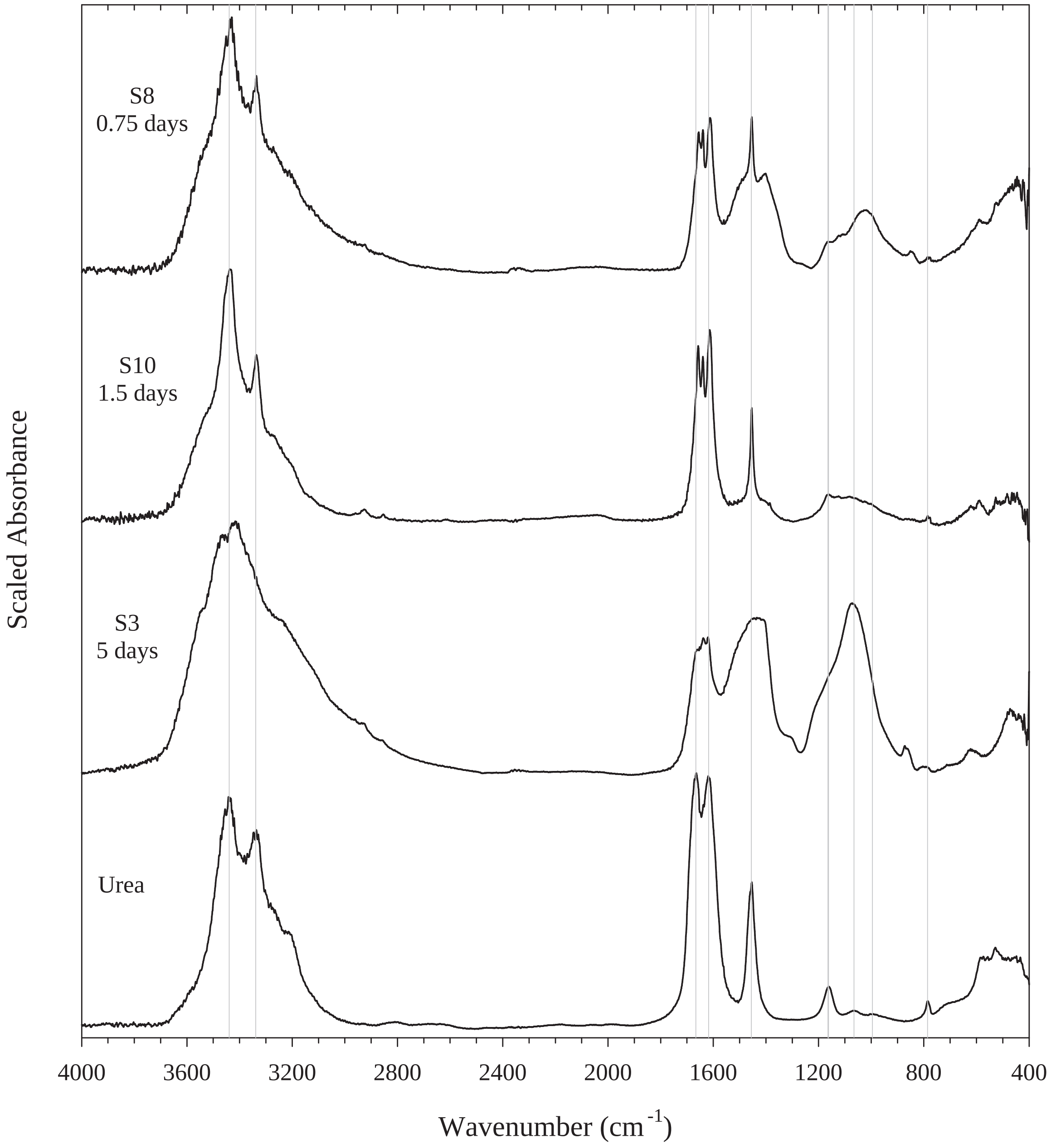

Fig. 6.—Mid-IR spectrum of the white powder remaining after the liquid from the cup was dried and ammonium carbonate removed from the first three experiments of the time evolution series (experiments S8, S10, and S3) compared with that of urea. Vertical lines mark the peak positions of urea.

TABLE 3

Peak Positions and Vibrational Modes of Urea

Peak Position (cm^{-1})	Vibrational Mode
3442	NH_2 a.s. stretch
3337	NH_2 s. stretch
1664	CO stretch
1638	NH_2 s. bend
1619	NH_2 a.s. bend
1454	CN a.s. stretch
1161	NH_2 s. rock
1064	NH_2 a.s. rock
992	CN s. stretch
785	CO o.p. bend

Note.—c.f. Figure 6. “a.s.” = antisymmetric, “s.” = symmetric, and “o.p.” = out of plane.

resembles that of a urea-water solution than that of a crystalline solid, even though the spectrum is of the sample in a KBr disk. The band strengths can also vary depending on the state of the urea in the sample. These observations may justify the claim that the differences in the spectra in Figure 6 do not reflect compositional differences, but rather the physical state of the sample.

There are some minor differences between these spectra and that of urea that merit attention. First, in the spectrum from S10, and to a lesser extent S3 and S8, there are weak peaks at 2937 and 2854 cm^{-1}. These are indicative of antisymmetric and symmetric aliphatic CH_2 streches. Although it is possible that these are due to CH_2 groups in the sample, they are probably due to pump oil backing into the bell jar in which these samples were dried. Second, in the spectrum of S8, there is a peak of medium intensity at 1401 cm^{-1}. This is probably not due to urea. It may be due to residual ammonium groups adhering to the sample after drying, or perhaps to a small amount of ammonium bicarbonate remaining in the sample.

Note that the broad band from 1550 to 1350 cm^{-1} in the spectrum from S3 extends this far and may share a common origin.

A residue also remained after drying the liquid and removing ammonium carbonate from experiments S17, S21 and S22 (see Table 1). The sample from S17 was a powder, but the samples from S21 and S22 were waxy, the former bright green and the latter brown in color. The mid-IR spectra of these samples are compared with that of urea in Figure 7. These spectra show some evidence for the presence of urea, but not as clearly as in Figure 6. For example, the spectrum from S22 has strong broad bands from 3600 to 2800 cm^{-1}, 1650 to 1600 cm^{-1}, and 1200 to 1000 cm^{-1} that are similar to those from S3 and peaks at 1454 and 1401 cm^{-1} that are similar to those in spectrum of S8. The spectrum from S21 is dominated by water. The band from 1150 to 1000 cm^{-1} is similar to urea, but the strong peaks in the spectrum of urea are either absent or covered by those of water. The spectrum from S17 is similar to that from S22 and may also contain a small amount of water. As above, the CH_2 stretches at 2937 and 2854 cm^{-1} are probably due to pump oil.

A very small amount of material ($\approx$0.1 mg) was also recovered from two of the control experiments: S7 and S13. The material from S13 was actually insoluble, but it is presented here due to its similarity to that from S7. The mid-IR spectra of these samples are shown in Figure 8. The sharp peaks in the spectrum from S13 are due to pyrene, which accounts for the insoluble nature of this sample. These spectra lack sufficient structure to characterize the nature of these materials with any certainty, but the broad bands from 3600 to 2800 cm^{-1}, 1700 to 1300 cm^{-1}, and 1200 to 900 cm^{-1} are similar to those in the spectrum from S3, shown in Figure 6. Both samples were dried and prepared together, at the same time but in different vials, so there may be some cross-contamination between samples.

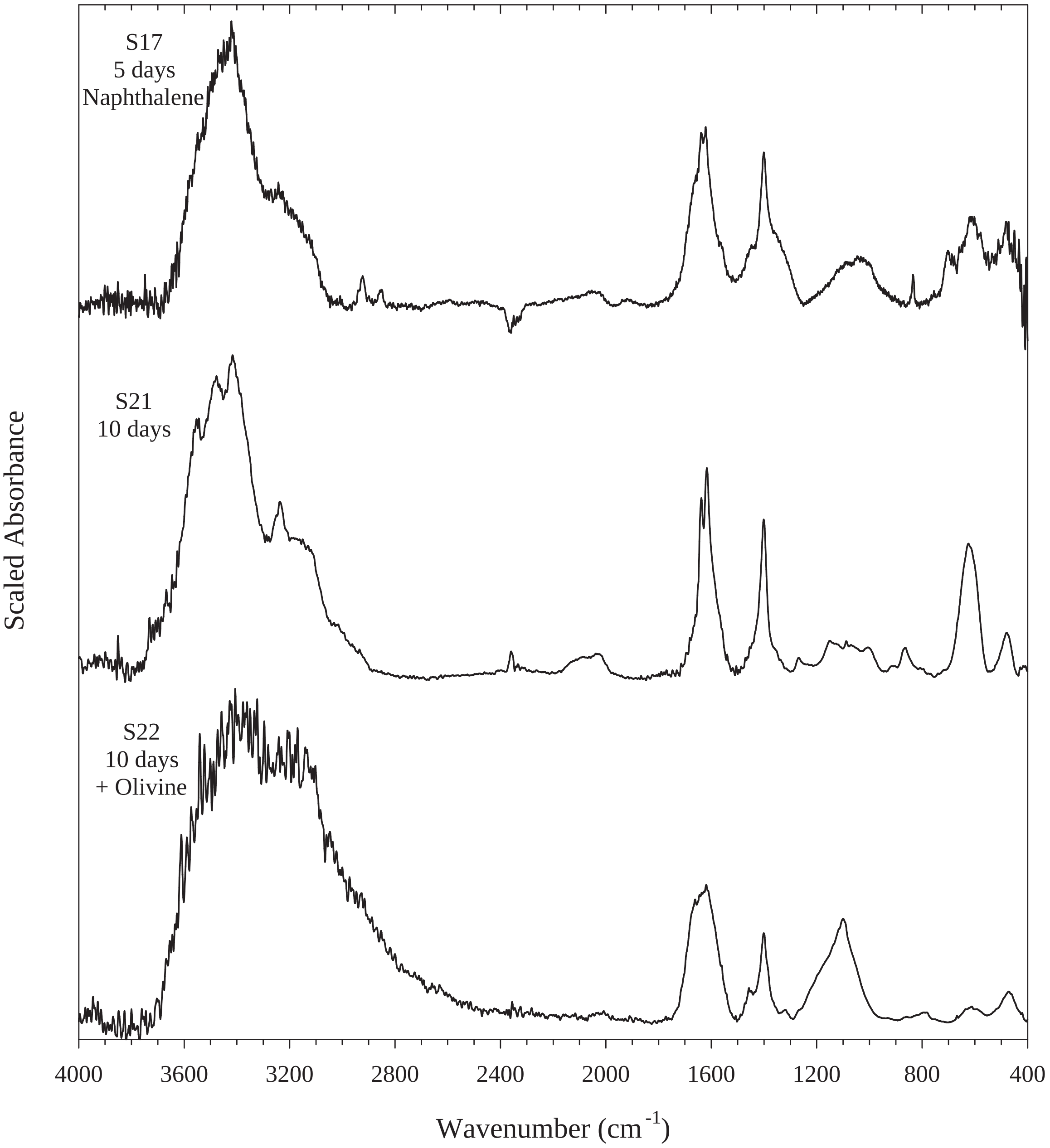

Fig. 7.—Mid-IR spectra of the material remaining after the liquid from the cup was dried and ammonium carbonate removed from experiments S17 (top), S21 (middle), and S22 (bottom).

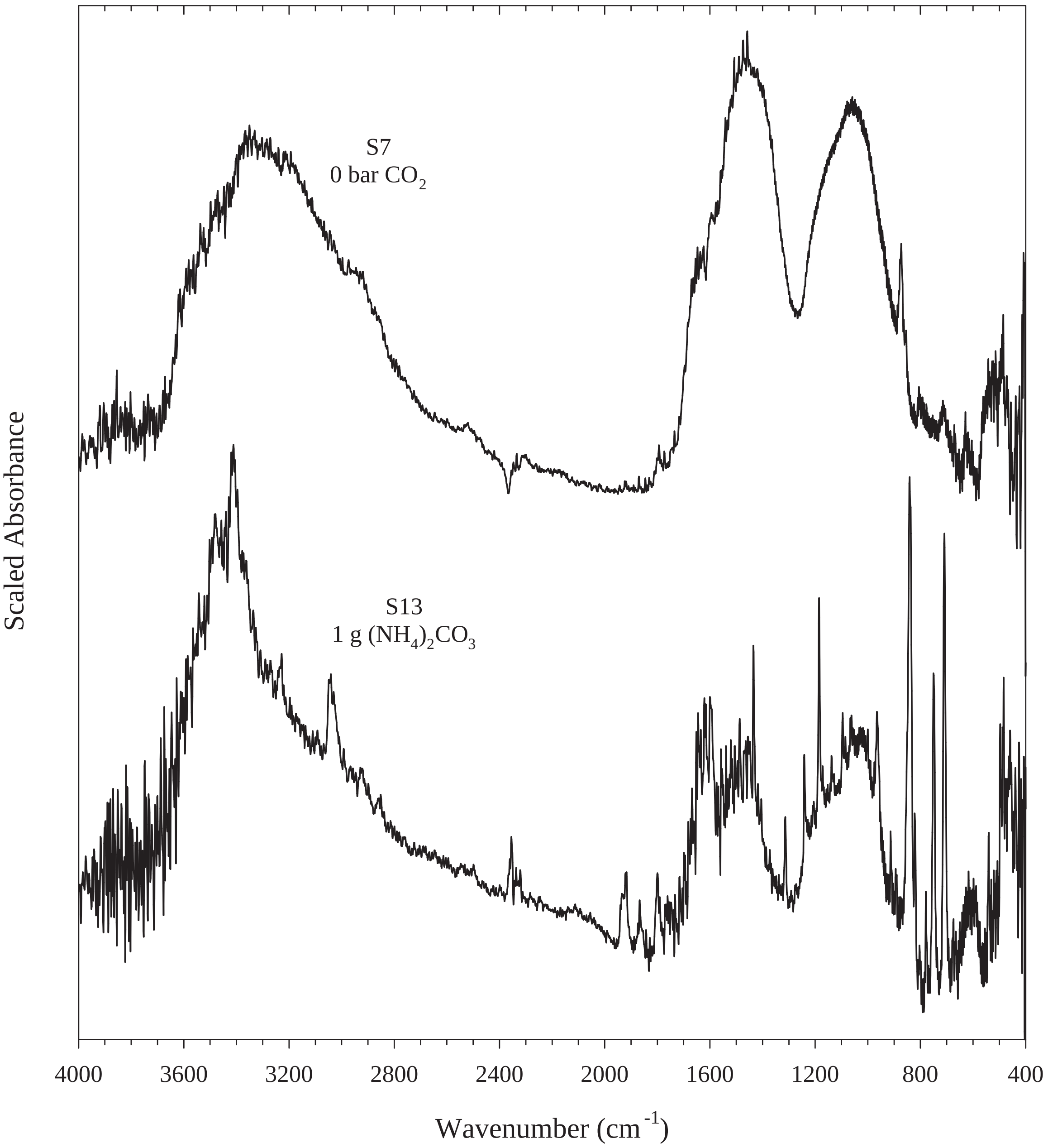

Fig. 8.—Mid-IR spectra of the white powder remaining after the liquid from the cup was dried and ammonium carbonate removed from experiments S7 (top) and S13 (bottom).

3.5 Insoluble Material from the Sample Cup and Vessel

A significant amount of insoluble material was collected in each of the experiments in the time evolution series. The amount of material collected was 0.1 mg, 3.5 mg, 14.3 mg, and 45.1 mg from experiments S10, S3, S12, and S21, respectively. The color of this material ranged from black and brown in S10 and S3 to green-brown in S12 and olive green in S21. The mid-IR spectra of these materials are shown in Figure 9. The spectrum of pyrene is shown at the top for reference, because this is the spectrum of the unaltered starting material. After 0.75 days (experiment S8), the sample is brown but there is no difference between this spectrum and that of pyrene, except, perhaps, a small additional amount of adsorbed water (note band from 3600 to 3300 cm^{-1}). By 1.5 days (experiment S10), the sample is black and its spectrum has changed. Pyrene is still clearly visible in the spectrum of this sample, but several clearly discernable new features have emerged. First, there is a very broad feature from 3600 to 2700 cm^{-1}. This band shows little structure, except for the CH strecth of pyrene at 3047 cm^{-1}. Next, there is a strong and broad feature from 1700 to 1250 cm^{-1}. This feature is split into two clear bands; one from 1700 to 1400 cm^{-1} and the other from 1400 to 1350 cm^{-1}. These bands, especially the former, are overlaid with several peaks due to pyrene, making it impossible to resolve any finer structure. There are two other noteworthy features of moderate intensity: a peak at 1086 cm^{-1} and a band from 1000 to 800 cm^{-1}.

After 5 days (experiment S3), there is almost no trace of pyrene remaining in the spectrum of the insoluble material and the features noted above are better resolved. The only indications that pyrene might still be present in some form are the three minor peaks at 850, 749, and 710 cm^{-1}, which would correspond its CH out-of-plane bending modes; however, this indentification is by no means certain. The spectrum then remains mostly unchanged, with only subtle differences, after progressing to 10 days (S12) and thence to 20 days (S21); however, there is one

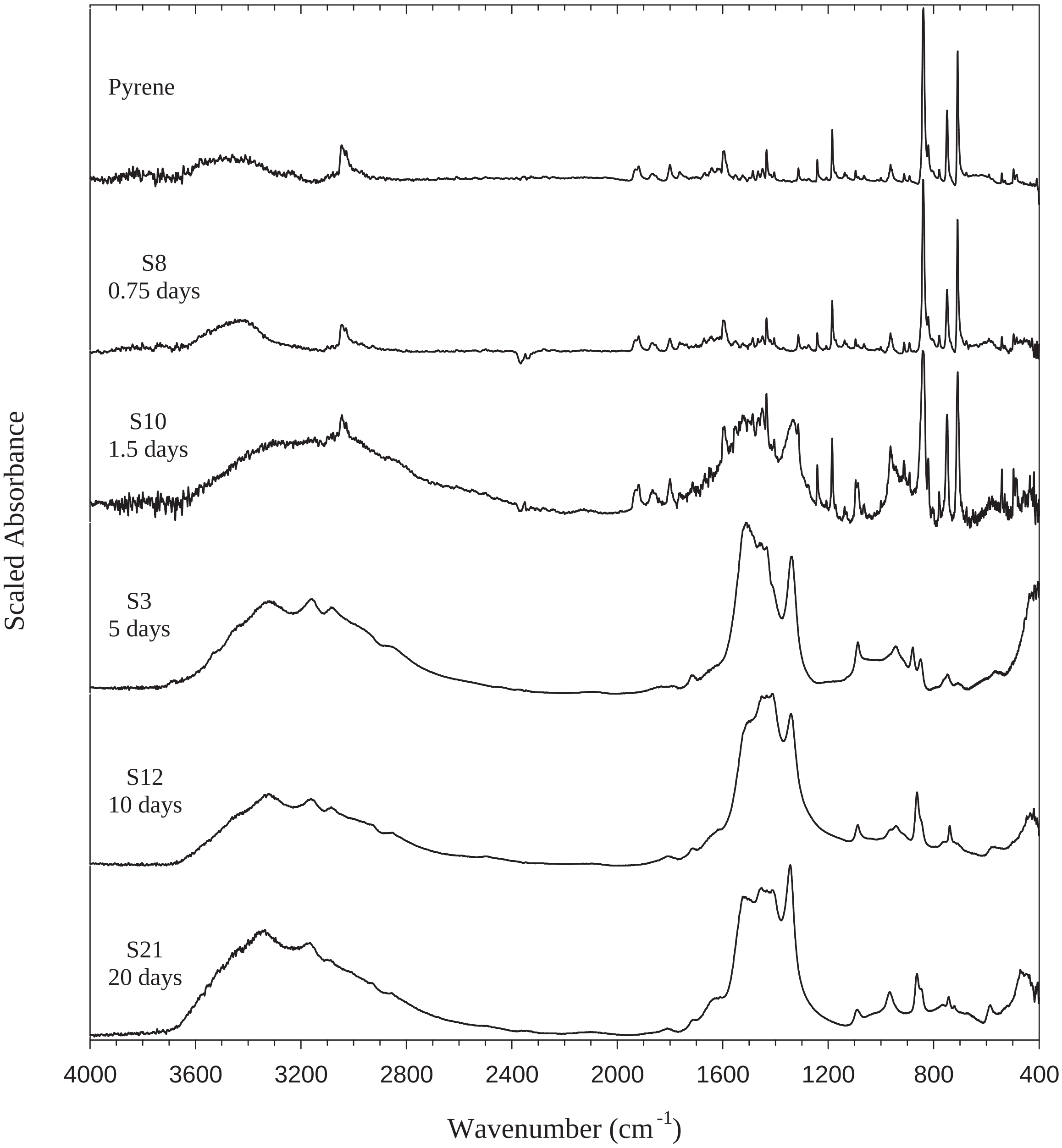

Fig. 9.—Mid-IR spectra of the insoluble material recovered from the sample cup in the time evolution series of experiments. The spectrum of pyrene is shown at the top for reference.

key exception. In the spectra from S12 and S21, three strong peaks appear. The strongest is at 1412 cm^{-1}; the two others are at 863 and 740 cm^{-1}. These peaks are due to siderite (iron carbonate, $FeCO_3$). Siderite was also found in the vessel (beneath the sample cup) in experiments S12, S21, and S23. Figure 10 shows the ratio of the mid-IR spectrum of the insoluble material from the cup in experiment S12 to that from experiment S3, the spectrum of the insoluble material from the vessel from experiment S23, and siderite. Note that the spectrum of siderite shows a significant amount of water at 3600 - 3200, 1650 -1600, and 619 cm^{-1}. Water is also evident in the spectrum from S23 and the ratio of the spectrum from S12 to that from S3, but in lesser amounts.

The presence of siderite in the insoluble material from the cup in experiment S21 was confirmed by Mössbauer spectroscopy. Figure 11 shows the Mössbauer spectrum of this material from S21 compared with that of natural siderite (from Wade et al., 1999). As the sample was cooled from 300 K to 16 K, the spectrum changes from that of a quadrapole doublet to that of a magnetic sextet with a transistion temperature of around 40 K. The sixth peak in the sextet occurs at around 5.2 mm s^{-1} and is only partly visible in the 16 K spectrum. Both the doublet at 300 K and the sextet at 16 K are characteristic of natural siderite. Note also that, in the spectrum from S21 at 300 K, the peak at around 0.2 mm s^{-1} is somewhat larger that the one at around 2 mm s^{-1} and has a small shoulder on its left side. This suggests the presence of an Fe^{+3} doublet on either side of the central siderite peak at around 0.2 mm s^{-1}. This Fe^{+3} doublet is also present in the spectrum from S21 at 16 K. The Fe^{+3} is probably present in the form of Fe_2O_3. It is possible that this Fe_2O_3 is visible in the mid-IR spectrum from S21; for example, Figure 12 shows a comparison between the mid-IR spectrum of S21 and that of Fe_2O_3 in the region 700 - 400 cm^{-1}. The similarity between these two spectra suggests

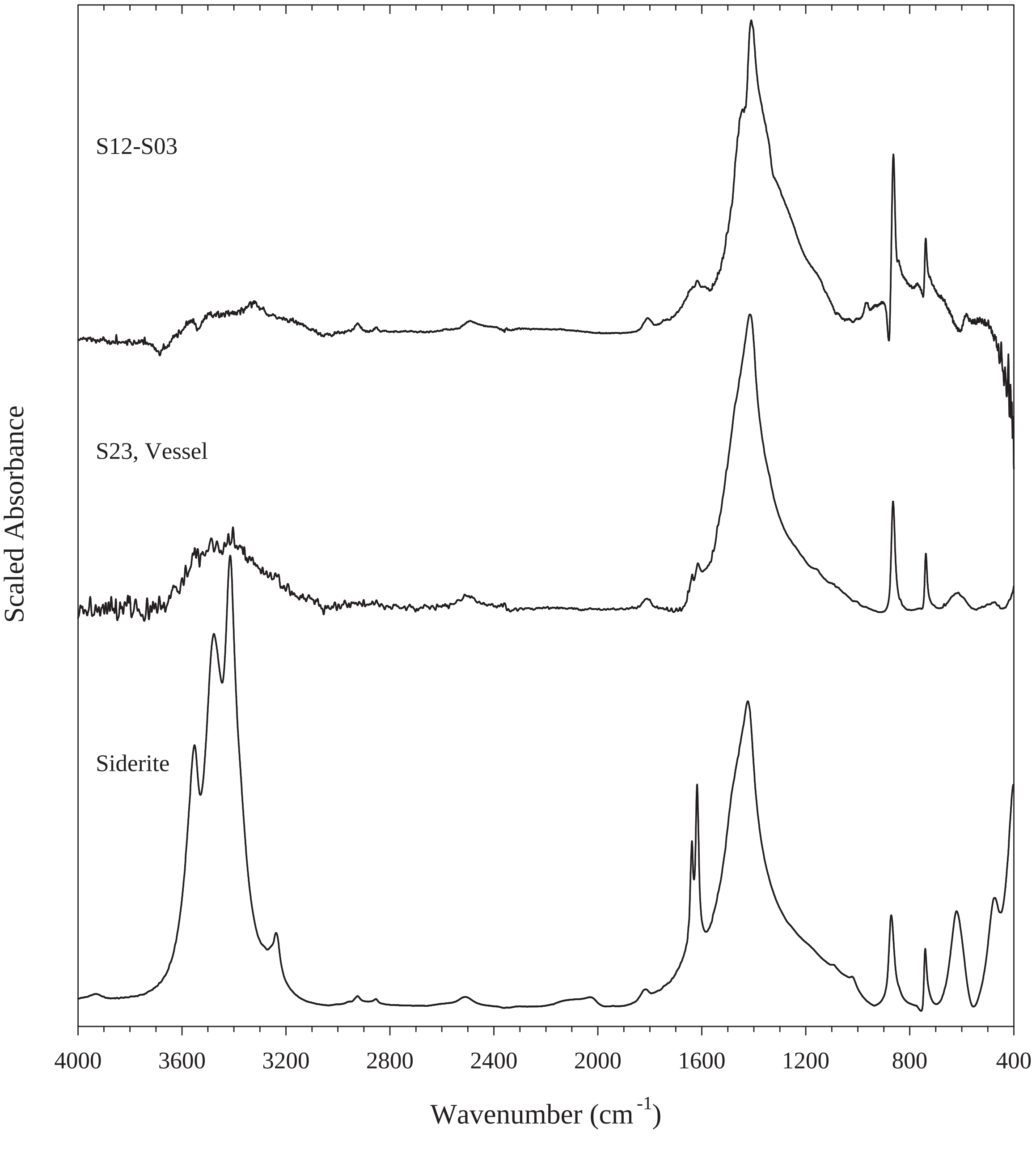

Fig. 10.—Ratio of the mid-IR spectrum of the insoluble material from experiment S12 to that from S3 (top) compared with the mid-IR spectrum of the insoluble material recovered from the vessel in experiment S23 (middle), where no pyrene was added, and that of siderite (bottom).

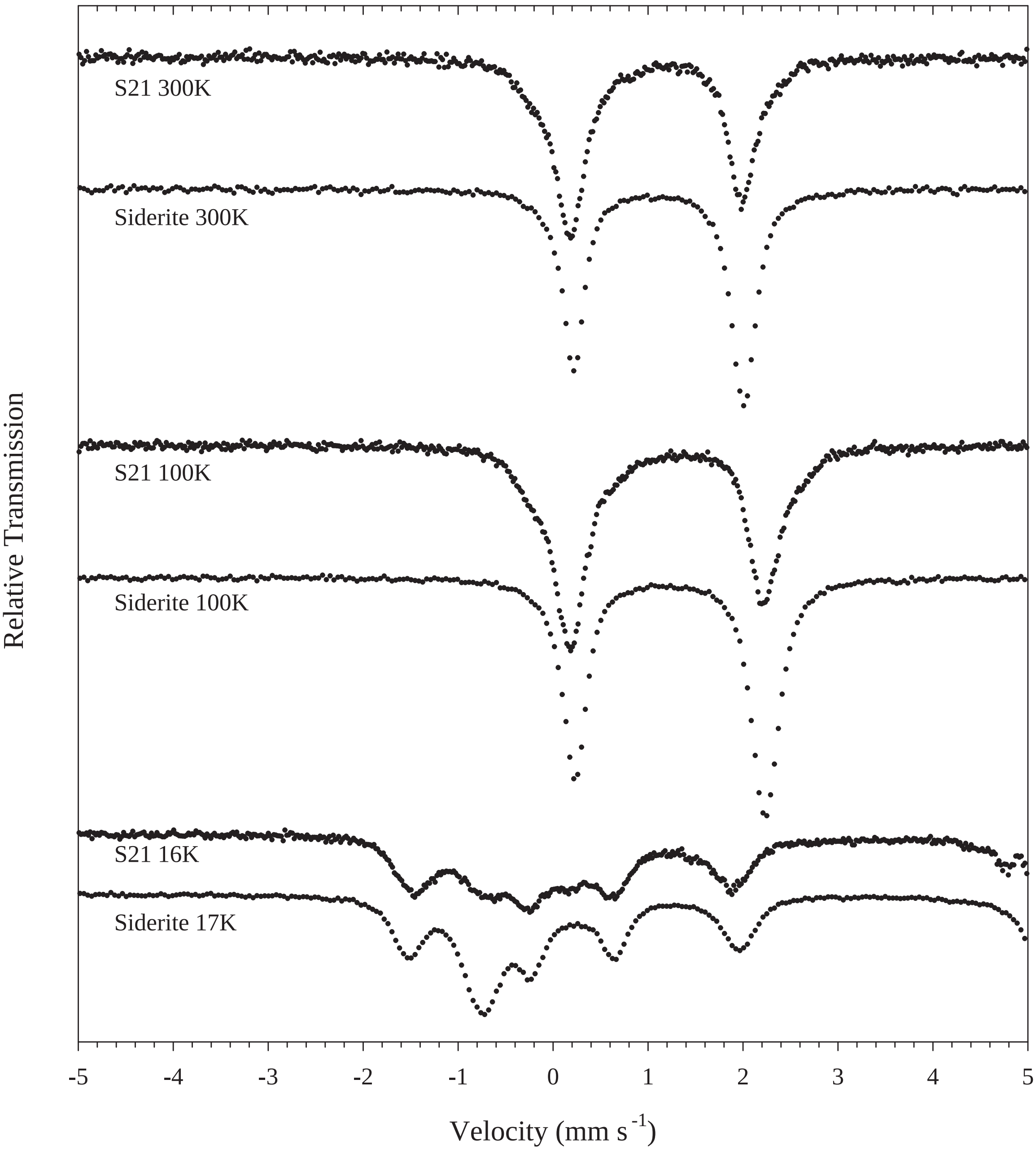

Fig. 11.—Mössbauer spectra of the insoluble material in the cup from experiment S21 compared with that of natural siderite at three different temperatures: 300 K, 100 K, and 16 K. The spectra of natural siderite were originally presented by Wade et al. (1999).

that Fe_2O_3 may be visible in the spectrum from S21; however, this identification cannot be asserted with confidence.

Aside from the production of siderite, the spectrum of the insoluble material from the cup remains fairly stable after 5 days. The remaining features are organic in origin, because the corresponding material is found when pyrene is present (e.g. experiments S3, S12, and S21) but is not found when pyrene is absent (experiment S23). The peak assignments described below are summarized in Table 4. Because the provenance of this material is pyrene, it is probably essentially aromatic in character. If so, it must be highly symmetric because, although the symmetric aromatic C=C stretching mode appears at around 1512 cm^{-1}, the anti-symmetric aromatic C=C stretching mode at around 1600 cm^{-1} is conspicuously absent. There is a band of moderate intensity from around 1640 to 1600 cm^{-1} that becomes better resolved with time (e.g. S21) and could be attributed, in part, to such an anti-symmetric C=C strecth, but it is much more likely that this is due to the OH bending modes of water adsorbed to or trapped within the insoluble material. Confirmation of an aromatic character can be made by assigning an aromatic CH stretching mode to the peak at 3086 cm^{-1}; however, this wavenumber is somewhat higher than the usual CH strecth of pyrene at 3045 cm^{-1}. The addition of aromatic N into the ring can increase the wavenumber of this peak position to around 3080 cm^{-1}. The presence of aromatic N can be confirmed by assigning the strong peak at 1341 cm^{-1} to an aromatic CN stretch.

The strong, wide band from 3600 to 2700 cm^{-1} suggests extensive hydrogen bonding, probably between the organic component and the carbonate cation of the siderite. The source of the hydrogen may be amine or hydroxyl groups attatched to the aromatic component. Evidence for this can be seen in the peaks at around 3325 and 3161 cm^{-1}. The former may be either an OH or an NH stretch. If it is due to an OH stretch, then the peak at 3161 cm^{-1} may mark the presence of NH_4^+;

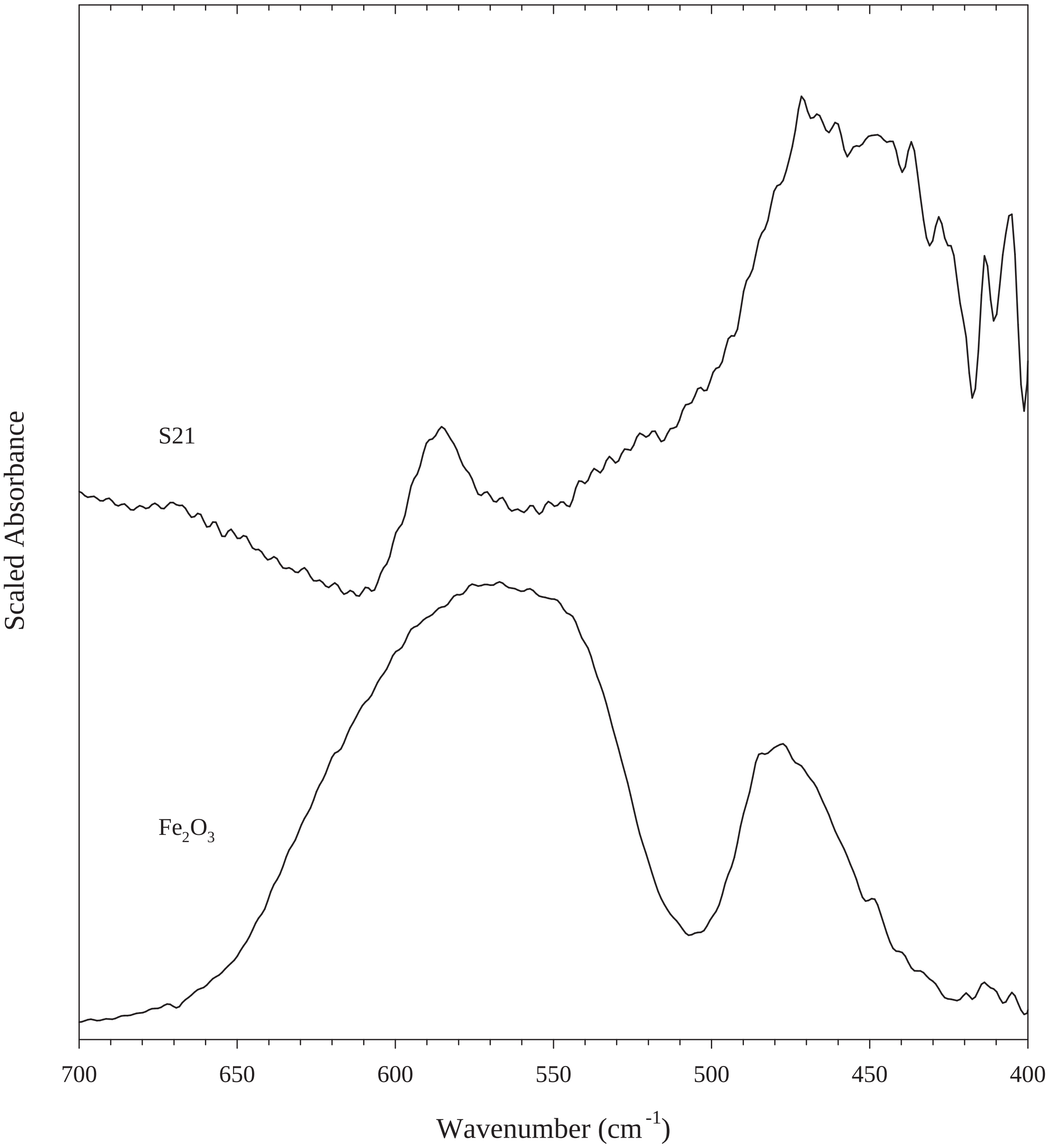

Fig. 12.—Mid-IR spectrum of the insoluble material from S21 (top) compared with that of Fe_2O_3 (bottom) in the region 700 - 400 cm^{-1}.

TABLE 4

Peak Positions and Vibrational Modes of the Insoluble Material From the Cup

Peak Position (cm^{-1})	Assigned Vibrational Mode
3325	NH_2 a.s. stretch
3161	NH_2 s. stretch
3086	aromatic CH stretch
1935	aliphatic CH_2 a.s. stretch
1855	aliphatic CH_2 s. stretch
1811	siderite
1713	aromatic overtone
1512	aromatic C=C s. stretch
1453	aromatic skeleton
1433	aromatic skeleton
1412	CO_3^{-2} a.s. strecth (siderite)
1341	aromatic CN stretch
1088	aromatic skeleton
967	aromatic skeleton
945	aromatic skeleton
879	unknown (aromatic CH o.p. bend?)
863	CO_3^{-2} o.p. bend (siderite)
850	aromatic CH o.p. bend
749	aromatic CH o.p. bend
740	CO_3^{-2} i.p. bend (siderite)
710	aromatic CH o.p. bend

Note.—c.f. Figure 9. “a.s.” = antisymmetric, “s.” = symmetric, “o.p.” = out of plane, and “i.p.” = in plane.

by comparison the spectra of ammonium carbonate and ammonium bicarbonate in Figure 4 show absorbtion at around 3127 cm^{-1}. If it is an antisymmetric NH_2 stretching mode, then the peak at 3161 cm^{-1} may be the symmetric NH_2 stretch. These wavenumbers are somewhat lower than that of the usual NH_2 stretch (c.f. urea, Table 3). This assignment may be justified if the amine group is hydrogen bonded to the carbonate cation; the hydrogen bond would lengthen the N-H bonds, making them vibrate at lower wavenumbers. If amine groups are present, the NH_2

bending modes in the 1650-1600 cm^{-1} region should be visible. As noted above, there is moderate absorbtion here in the spectrum from S21; however, this region is mostly empty in the spectra from S3 and S12, so it is probably not attributable to the NH_2 bending modes. Hydrogen bonding should shift the NH_2 bending modes to lower wavenumbers as it would the NH_2 stretching modes. If this is the case, these peaks may appear below 1600 cm^{-1}, possibly merged with the symmetric aromatic C=C stretch at 1512 cm^{-1}.

The region from 3600 to 2800 cm^{-1} in the spectra from S3, S12, and S21 is shown in greater detail in Figure 13. All three spectra have been scaled to their absorption at 1512 cm^{-1}. The entire band in this region grows in intensity with time, suggesting increased hydrogen bonding. Water adsorbed to the the sample probably accounts for most of this increase. The intensity of the peak at 3325 cm^{-1} increases relative to this underlying band, but the intensity of the peak at 3161 cm^{-1} remains constant. The increase in the intensity of the first peak can be explained by increased water adsorption, which would peak at around 3500 cm^{-1}. If this accounts for all of the increase, then the peaks at 3352 and 3161 cm^{-1} may share a common origin; for example, the NH_2 stretching modes. Not all of this increased absorption need be attributed to the OH stretch of hydrogen-bonded water. Some portion of it may be due to the OH stretch of hydroxyl groups bound to the aromatic material. Probably, the reality is a mixture of these three possibilities: adsorbed water, NH_2 groups, and OH groups.

The intensity of the peak at 3086 cm^{-1} decreases with time. This indicates a decrease in the amount of aromatic C-H bonds. This may be due to either a change in aromaticity or a substitution of aromatic hydrogen. The former could indicate either ring cracking or hydrogenation, both of which would be accompanied by an increase in aliphatic CH stretches between 3000 and 2850 cm^{-1}. There is a plateau in the intensity of the broad band between around 2900 and 2850 cm^{-1} and a point

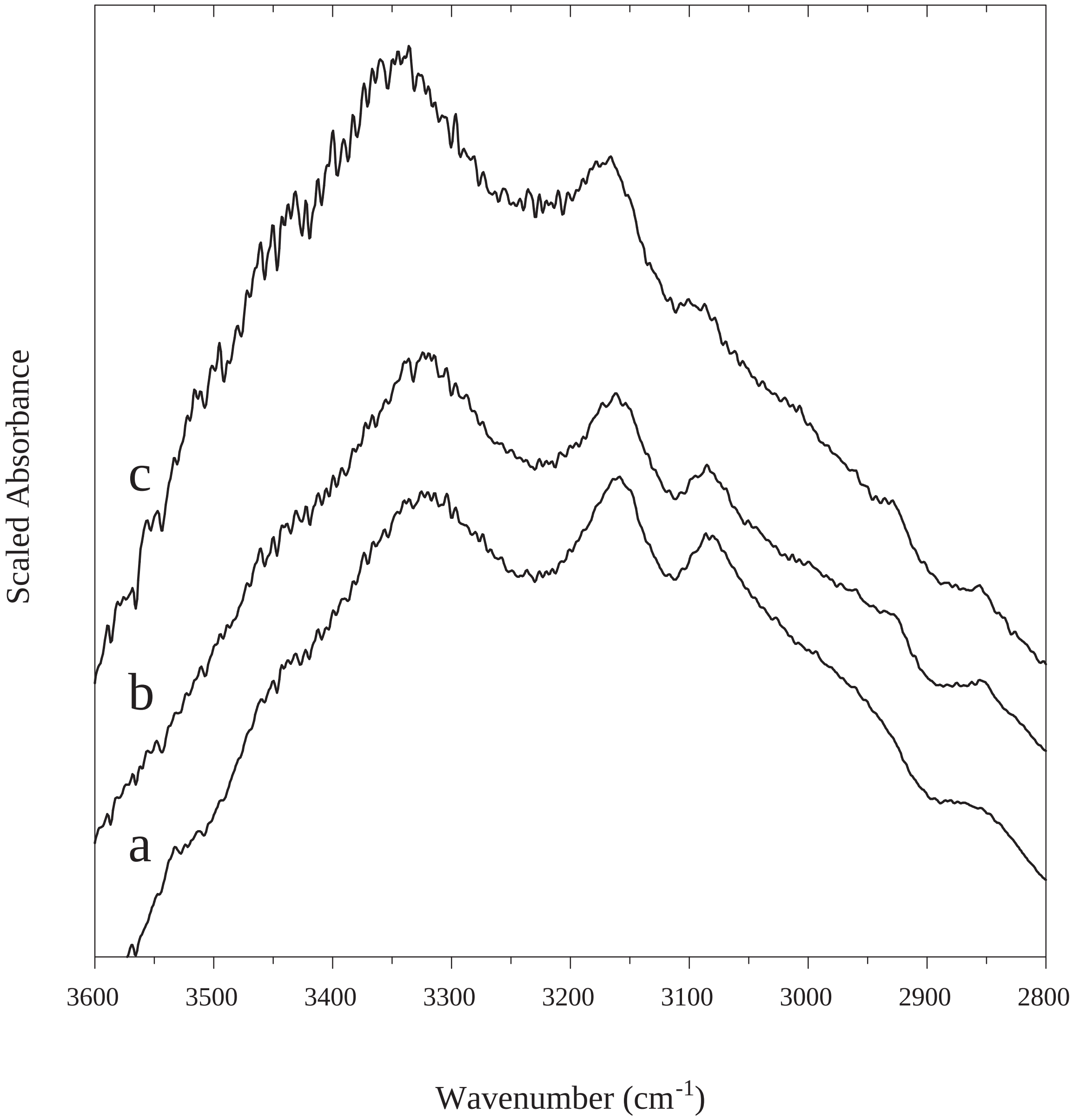

Fig. 13.—Mid-IR spectrum of the insoluble material in the cup from (a) S3 (5 days), (b) S12 (10 days), and (c) S21 (20 days) in the 3600 - 2800 cm^{-1} region. All three spectra have been scaled to their absorption at 1512 cm^{-1}.

of inflection at around 2930 cm^{-1}. The point of inflection develops into a narrow plateau from around 2950 to 2930 cm^{-1} and small peaks develop at around 2855 and 2935 cm^{-1} in the spectra from S12 and S21. These features indicate the presence of aliphatic CH stretching, but they are quite subdued. The small peaks may indicate that most of the absorption is from CH_2 groups. As with the soluble material, these peaks may be due to pump oil backing into the bell jar while drying; however, the plateaus themselves indicate broadening by hydrogen bonds and therefore originate from the insoluble material. The appearance of the plateaus may indicate the lack of CH_3, because this group tends to absorb at higher wavenumbers (around 2870 and 2965 cm^{-1}). The lack of CH_3 may favor hydrogenation rather than ring cracking, unless the cracked rings are being terminated by something other than hydrogen. The lack of apparent aliphatic C=C bonds near 1650 cm^{-1} may also constrain the extent of ring cracking. It is important to note that a similar plateau appears in the spectrum of ammonium carbonate in Figure 3, where no C-H bonds are present. Likewise, this plateau in the spectra of the insoluble material may arise from hydrogen bonding; however, in this case, the shape of the band and the likelihood of aliphatic C-H bonding make that interpretation less plausible.

The region from 1800 to 600 cm^{-1} in the spectra from S3, S12, and S21 is shown in greater detail in Figure 14. Again, all three spectra have been scaled to their absorption at 1512 cm^{-1}. As noted above, the peaks at 1512 and 1341 cm^{-1} may be a symmetric aromatic C=C stretch and aromatic CN stretch respectively. The absence of an antisymmetric aromatic C=C stretch implies that the aromatic ring must be highly symmetric, possibly no larger than benzene. Larger ring structures cannot be ruled out, but the absence of an antisymmetric C=C vibriational mode severly contrains the possibilities; as above, the molecule must be highly symmetric.

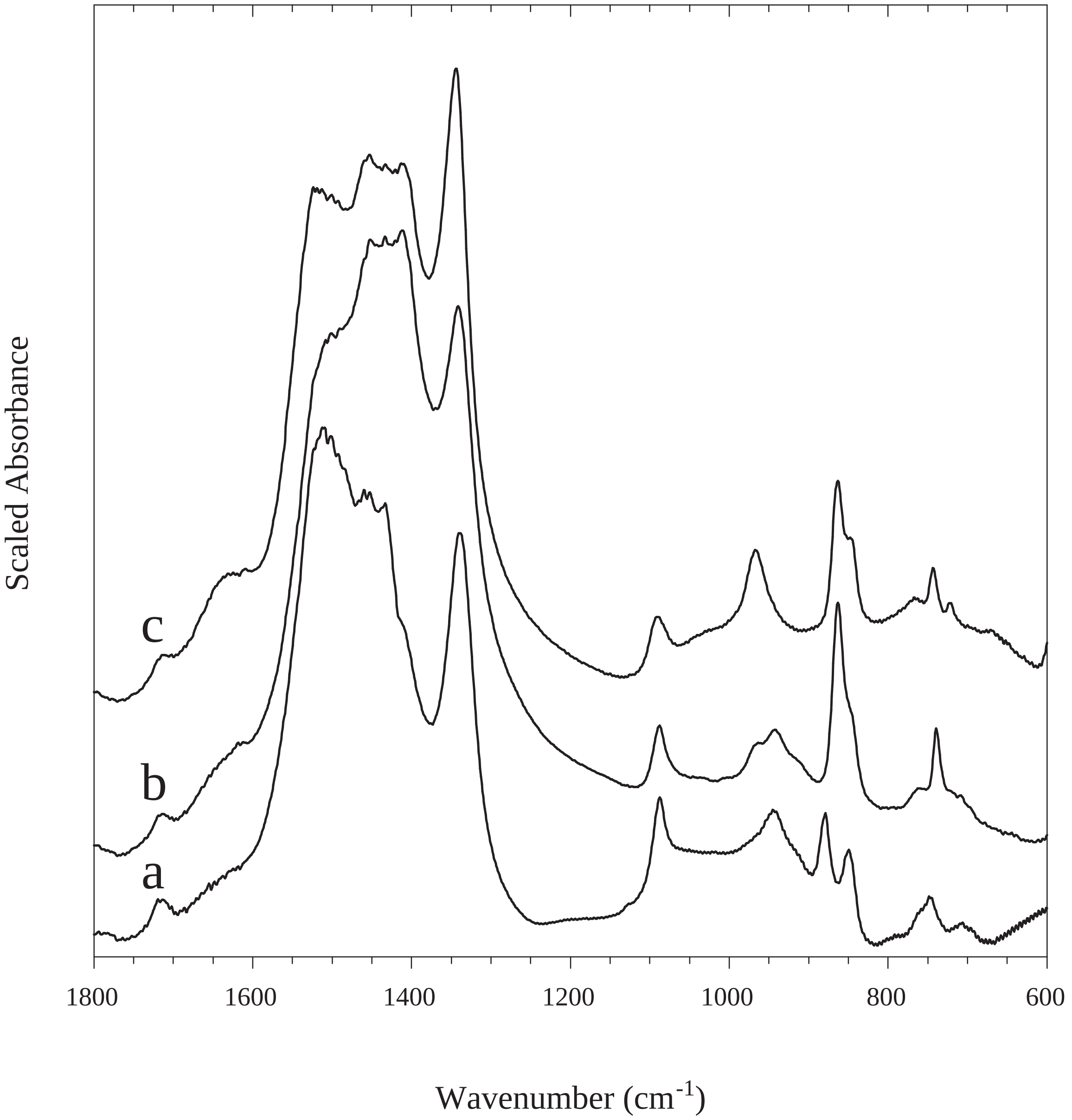

Fig. 14.—Mid-IR spectrum of the insoluble material in the cup from (a) S3 (5 days), (b) S12 (10 days), and (c) S21 (20 days) in the 1800 - 600 cm^{-1} region. All three spectra have been scaled to their absorption at 1512 cm^{-1} and offset for clarity.

All three spectra have a small peak at 1713 cm^{-1}. This would usually suggest the presence of carbonyl groups in the sample; however, absorption by C=O is usually very strong. If this peak is due to a C=O stretch, its position would indicate a ketone, carboxylic acid, or amide. The strength of the peak would imply that only a very small amount was produced. The fact that this peak is weak suggests a second possible assignment; it may be an overtone of the aromatic vibrational modes.

The band from 1640 to 1600 cm^{-1} grows with time. The growth of this band may indicate increased water adsorbed to the sample, or it may indicate increased substitution of aromatic H by NH_2. The fact that the aromatic CH stretch decreases in intensity may indicate the latter; however, the NH_2 bending modes are usually stronger than they are in the spectrum of S21 in Figure 14.

There are two minor features at 1453 and 1433 cm^{-1} within the strong band from around 1600 to 1100 cm^{-1}. These peaks do not change in intensity relative to that at 1512 cm^{-1}, possibly indicating that they are related to the aromatic skeleton. The first of these peaks happens to coincide with the CN stretch of urea, but cannot be identified from these spectra.

Beyond this strong band, there are several peaks that warrent a brief discussion. First, there is a peak at 1088 cm^{-1}. This peak becomes weaker with time. The positon of the peak is consistent with an aliphatic CN or CO stretch, but there is no other significant evidence for an aliphatic constituent. This peak coincides with the strong, broad absorption found in spectra of the soluble fraction (c.f. Figures 6 and 7), but the quality of the feature is very different in this case. This feature was attributed to the antisymmetric NH_2 rocking mode of urea in the soluble fraction, but the corresponding symmetric NH_2 rock around 1161 cm^{-1} is missing here. It is more likely that this feature, as well as the feature appearing at 945 cm^{-1} in the spectrum of S3 are associated with vibrations of the aromatic skeleton. This feature decreases in strength from S3 to S12 and is not present in the spectrum of S21. At the same time, a new peak at 967 cm^{-1} appears beside the peak at 945 cm^{-1} in the spectrum of S12 and grows in intensity in the spectrum of S21. The similarity in position between these two peaks suggests a common vibrational mode, and the gradual appearance of one at the expense of the other suggests a slow transformation from one configuration of the aromatic molecule to another.

Finally, there are three small peaks at 850, 749, and 710 cm^{-1} that do not appear to vary significantly in position or strength in the spectra. These peaks appear beneath the out-of-plane and in-plane bending modes of the carbonate cation of the siderite in the spectra of S12 and S21. These peaks are probably due to aromatic CH bending modes. There is one additional peak in the spectrum of S3 at 879 cm^{-1} that does not appear in the spectrum of S12 or S21. Neither does this peak appear in the spectrum of pyrene or S10. It may be due to a transient component of the material, perhaps an aromatic CH out of plane bending mode, but its origin is unknown.

Two possible structures for the insoluble organic material that are consistent with these assignments are phenazine ($C_{12}H_8N_2$) and benzo[a]phenazine ($C_{16}H_{10}N_2$). The spectra of these two aromatic compounds (from Coblentz Society, Inc., 2005) are compared with the difference of the spectra from S21 and S23 in Figure 15. This subtraction effectively removes the peaks of siderite and allows a more direct comparison with the spectrum of the insoluble material. The peak positions of both phenazine and benzo[a]phenazine are very similar to those of the subtracted spectrum in the 1600-800 cm^{-1} region, indicating that they may have similar structures. Indeed, the spectra of phenazine and benzo[a]phenazine are very similar to each other, differing mainly in the relative strengths of their major peaks. This suggests that larger structures containing the basic phenazine stuc-

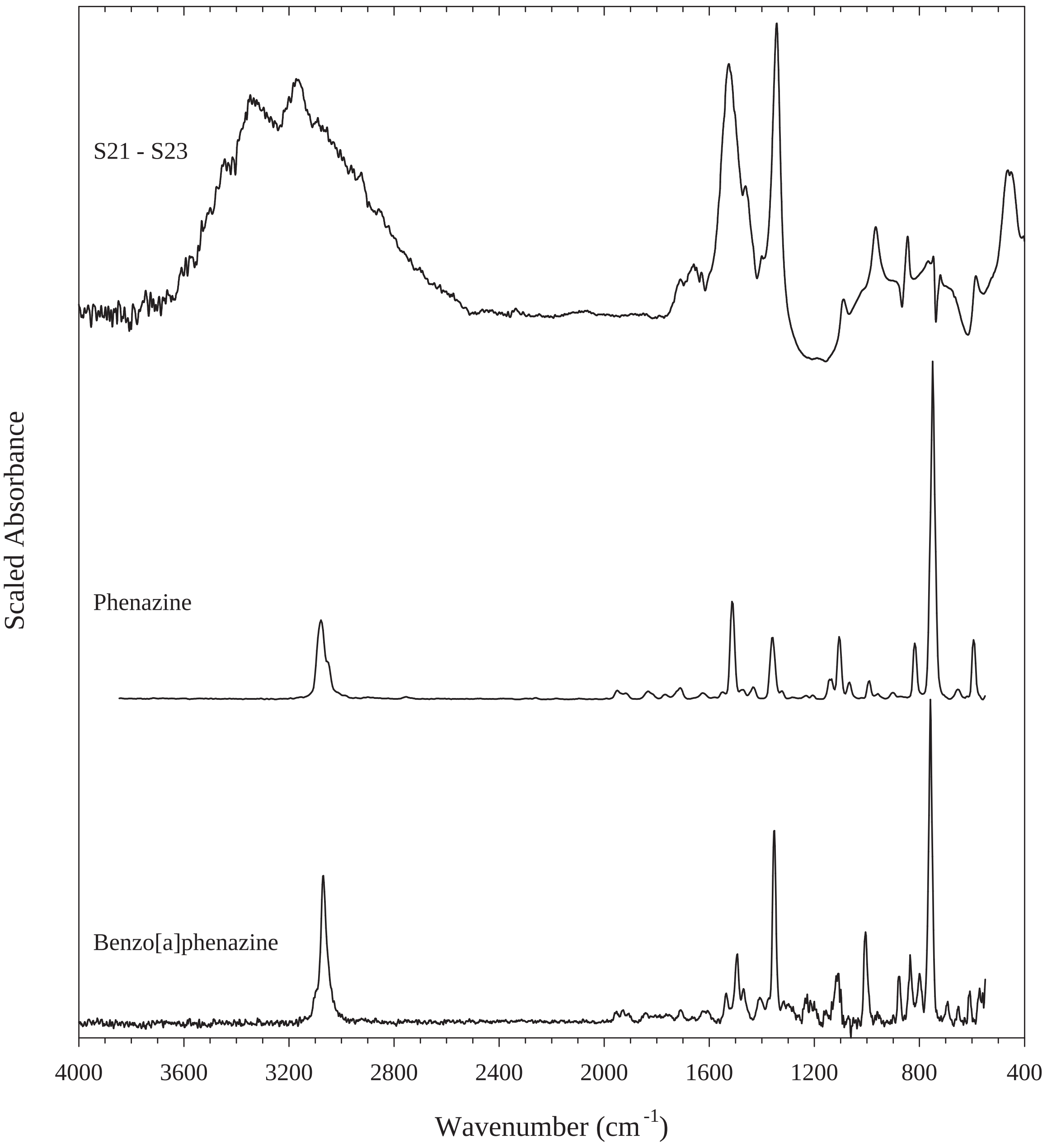

Fig. 15.—Ratio of the mid-IR spectrum of the insoluble material from S21 to that from S23 (top) compared with the mid-IR spectra of phenazine (middle) and benzo[a]phenazine (bottom). Reference spectra from Coblentz Society, Inc. (2005).

ture, i.e. two aromatic ring systems joined by two hetercyclic nitrogen atoms in the manner of phenazine, may be consistent with the spectra of the insoluble material. For example, phenazine may be considered to be two benzene rings joined by two aromatic nitrogen atoms to form a three-ring N heterocycle. One possiblility for the structure of the insoluble material that cannot be ruled out is that two pyrene structures may be joined in this manner. It is conceivable that a polymeric macromolecule could be constructed in this fashion; however, it is not possible to characterize the insoluble organic material as either more or less complex than pyrene from the available data.

Outside the 1600-800 cm^{-1} region in the spectra shown in Figure 15, absorptions due to the aromatic CH stretching mode near 3079 cm^{-1} and the aromatic out of plane CH bending modes below 800 cm^{-1} are much stronger relative to the aromatic CN stretching mode at 1341 cm^{-1} than those of the insoluble organic material, though the positions of these peaks are very similar. On the other hand, peaks assigned to CH_2, NH_2, and OH stretching modes are present in the difference of the spectrum of S21 and S23. This may be explained by hydrogenation and substitution of aromatic CH, although the corresponding bending modes are not apparent.

One experiment was performed where naphthalene was used instead of pyrene. A small amount of insoluble material was collected from this experiment, labeled S17. The mid-IR spectrum of this material is compared with that of the insoluble material from S3 in Figure 16. The peak positions in these two spectra are all the same, with three minor exceptions. First, there are two strong peaks at 3470 and 3411 cm^{-1} that are due to water in the KBr disk. Second, the broad band from 3600 to 2700 cm^{-1} in the spectrum of S17 lacks the structure apparent in that of S3. These first two differences are due to the small sample size in the KBr disk. This is probably also responsible for the slight differences in peak shape

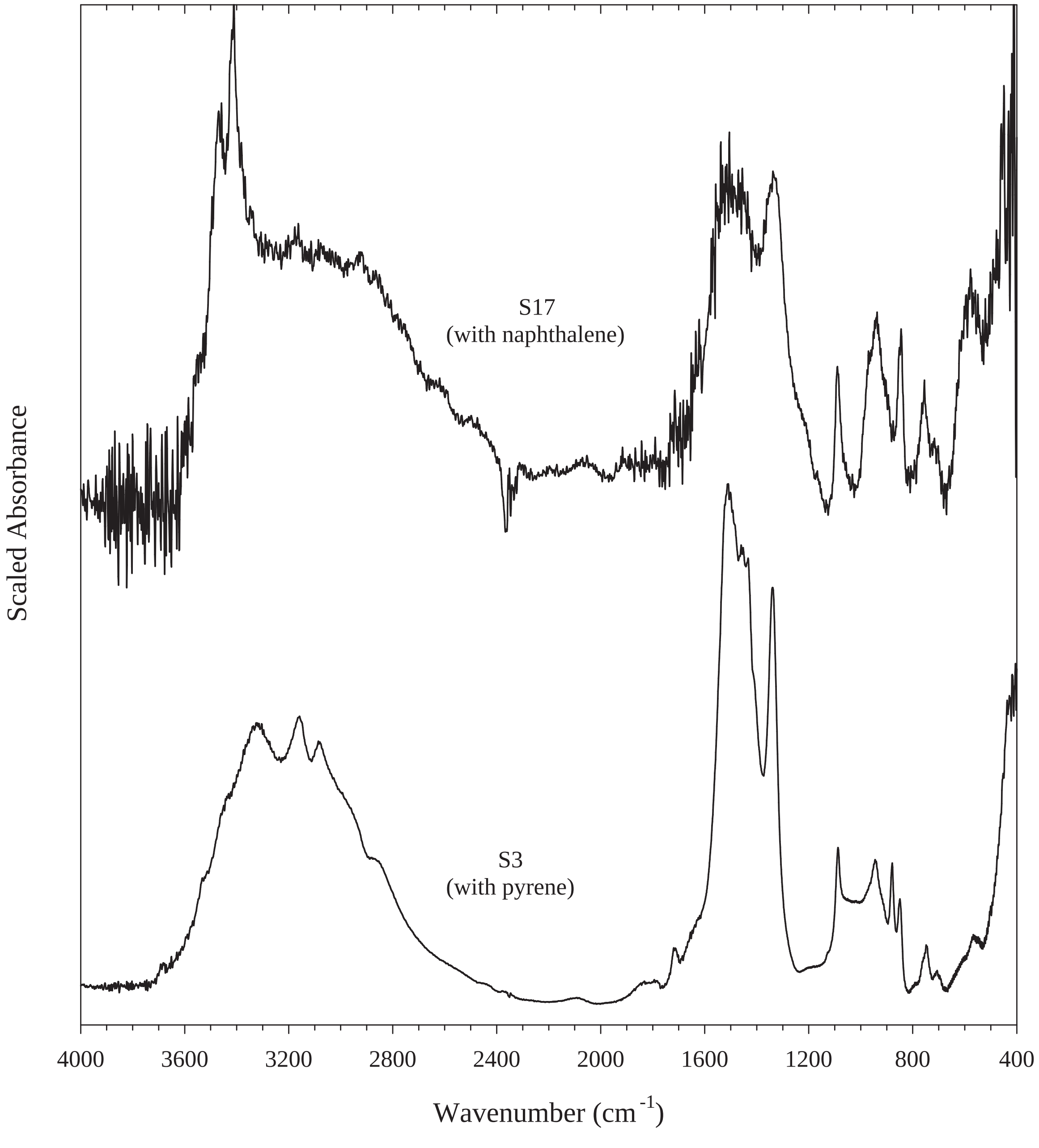

Fig. 16.—Mid-IR spectrum of the insoluble material in the cup from experiment S17, in which the PAH naphthalene was used instead of pyrene (top), compared with that from S3 (bottom). Both spectra have been scaled to their absorption at around 1341 cm^{-1}.

and strength throughout this spectrum. The third minor difference is the presence of the peak at 879 cm^{-1} in the spectrum of S3 and its absence in that of S17. This peak is of unkown origin and only appears in the spectrum of S3 in the time evolution series of experiments. The similarity bewteen these two spectra suggests that the choice of PAH may not be very important in determining the nature and structure of the organic component of the insoluble material.

One experiment (S22) was performed where the mineral olivine was included in the sample cup, but was otherwise identical to S12. This experiment yielded 0.7 mg of a black insoluble material that was found just above the water level in the sample cup. The mid-IR spectrum of this material is compared with that from experiment S12 in Figure 17. There are two important differences between these two spectra. First, peaks due to siderite are strong in the spectrum from S12 but are absent in the spectrum from S22. Second, the peaks at 1512, 1341, and 945 cm^{-1} in the spectrum from S12 are missing from the spectrum of S22. These two peaks are characteristic of the organic insoluble material from the time evolutions series of experiments (where olivine was absent). On the other hand, the broad band from around 3700 to 2800 cm^{-1} in the spectrum from S22 has peaks in roughly the same positions as that in the spectrum from S12; however, the aromatic CH stretch at 3086 cm^{-1} in the spectrum from S12 is missing in the spectrum from S22 and the aliphatic CH stretches at 2922 and 2852 cm^{-1} are stronger and better resolved in the spectrum from S22 than those in the spectrum from S12. Because the insoluble material from S22 was not dried in vacuum, there was no chance for contamination by pump oil, so the aliphatic CH strecthes arise from the sample.

The strong, prominent peaks at 1486 and 1432 cm^{-1} in the spectrum from S22 are also present in the spectrum from S12, but they are obscured by a strong, broad feature (c.f. Figure 14.) These peaks may also be aromatic in origin; how-

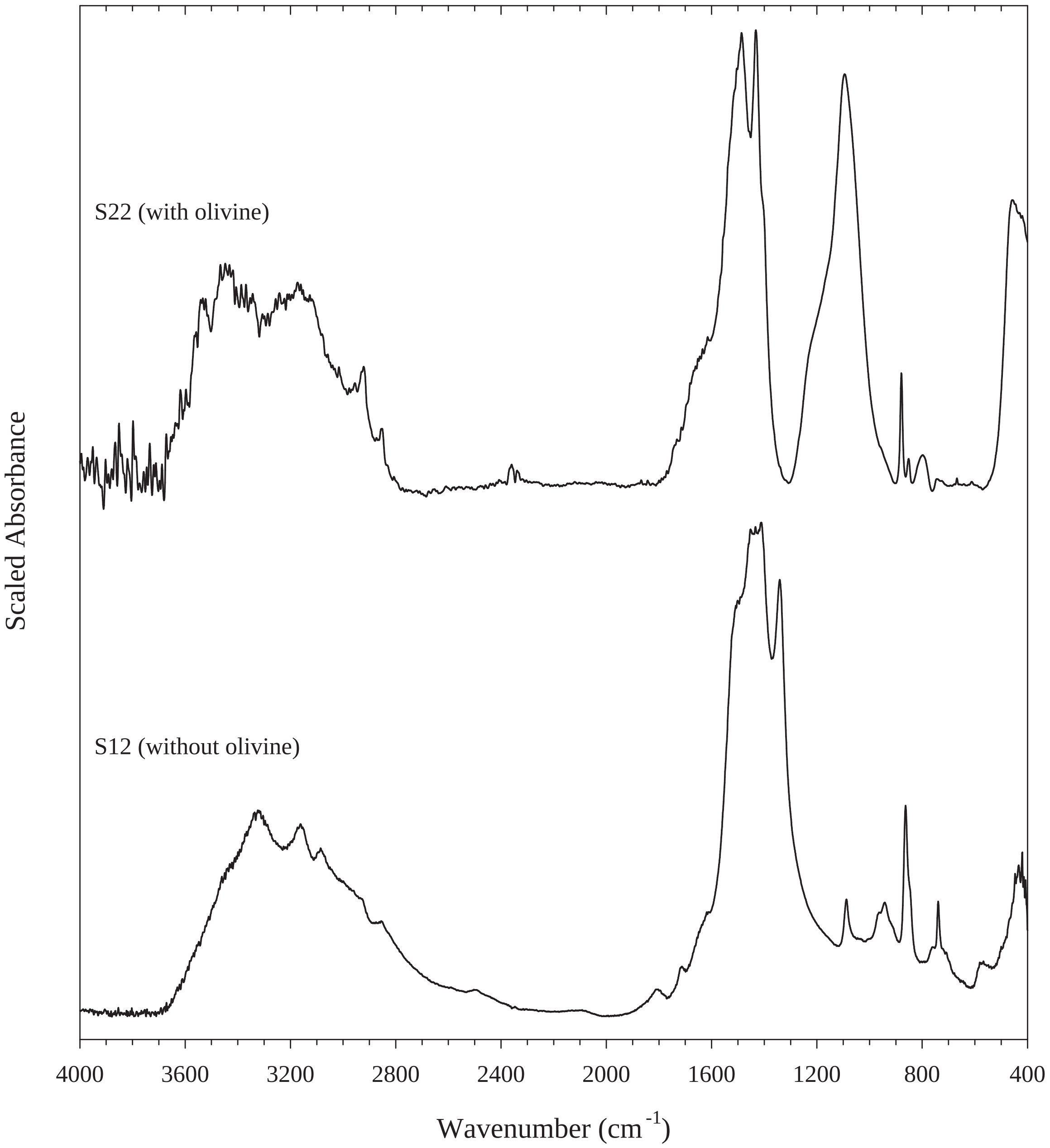

Fig. 17.—Mid-IR spectrum of the insoluble material in the cup from experiment S22, in which the mineral olivine was added (top), compared with that from S12 (bottom).

ever, like the organic insoluble material produced in the absence of olivine, the lack of strong absorption around 1600 cm^{-1} indicates a highly symmetric compound. There is a broad band from around 1700 to 1600 cm^{-1} in the spectrum from S22 that may be due, at least in part, to an antisymmetric aromatic C=C stretch. This band is also indicative of NH_2 bending modes and the OH bending modes of water. There is a small shoulder to this band at around 1715 cm^{-1} that is similar to the weak peak at 1713 cm^{-1} in the spectra from the time evolution series of experiments. The absence of a peak near 1341 cm^{-1} suggests that, if the material is essentially aromatic in nature, it probably does not contain heterocyclic nitrogen.

The strong, broad feature from around 1300 to 1000 cm^{-1} is identical to the same feature in the spectra of the soluble material, particularly the spectrum from S3 in Figure 6. This feature in the spectra from the soluble material was attributed to the NH_2 rocking modes of urea. There is no indication that urea is present in the spectrum of the insoluble material from S22, but this feature may still be due to NH_2 rockng modes. It may also indicate aliphatic CC, CN, and CO stretching modes. The remaining peaks at 879, 851, 798, and 743 cm^{-1} are similar to the peaks at 879, 850, and 749 cm^{-1} in the spectra of the insoluble material from the time evolutions series of experiments. Note that the peak at 879 cm^{-1} appears in the spectrum of the insoluble material from S22. Of the spectra from the time evolution series of experiments, this peak only appeared in that of S3.

The insoluble material from S22 is probably a hydrogenated aromatic compound with amine and hydroxyl groups. A similar material is probably present to a lesser extent in the organic insoluble material from the time evolution series of experiments, where a symmetric nitrogen heterocycle may comprise most of the material. The presence of the peak at 879 cm^{-1} in the spectrum of S22 may suggest that the insoluble material from this experiment represents a transient, intermediate compound in the production of the nitrogen heterocycle in the time evolution series of experiments, where olivine was not present. It may be that the presence of olivine inhibits the formation of this heterocycle. The lack of siderite suggests that olivine also inhibits the corrosion of the reaction vessel.

3.6 Altered Mineral from Experiment S22

The olivine used in experiment S22 was originally light olive green in color. After the experiment, the mineral was light tan. The mid-IR spectra of the altered mineral and the original, unaltered olivine are shown in Figure 18. The broad bands from around 3800 to 3200 cm^{-1} and 1650 to 1600 cm^{-1} are due to water. These bands are much more intense in the spectrum of the altered mineral than in that of the unaltered olivine, indicating that the altered mineral has bound water. The strong band centered around 1000 cm^{-1} is due to silicate stetching modes. This band is somewhat broader in the spectrum of the altered mineral but the peak positions remain unchanged. The peak at 883 cm^{-1} seems to have become somewhat less intense relative to the peak at 983 cm^{-1} and the entire band has become somewhat less intense than the peaks below 700 cm^{-1} in the spectrum of the altered mineral. The peak at 607 cm^{-1} is more intense relative to the other peaks below 700 cm^{-1} in the spectrum of the altered mineral due to absorbtion by water at around 620 cm^{-1}. The only significant difference in peak positions in the spectrum of the altered mineral is the appearence of the peak at 471 cm^{-1}, which does not appear in the spectrum of the unaltered olivine.

The broadening of the band centered around 1000 cm^{-1} may be explained by hydrogen bonding between absorbed water and the silicates. The appearance of the peak at 471 cm^{-1} suggests that the olivine has begun to transform, but the altered mineral appears to be essentially the same at the unaltered olivine. If the olivine was altered, it is not possible to say what it has become from these spectra.

Mössbauer spectroscopy was performed on the olivine and the altered mineral to further characterize any changes that may have occurred. The Mössbauer spectra of the altered mineral and the unaltered olivine are shown in Figure 19. These two spectra are identical, indicating that, if the mineral has changed, iron was not involved. The two peaks at -0.44 mm s^{-1} and 2.39 mm s^{-1} are indicative of the quadrapole splitting in olivine. The shoulders near 0 mm s^{-1} and 2 mm s^{-1} indicate that a small amount of pyroxene, perhaps enstatite ($(Mg,Fe)SiO_3$), was present in the unaltered olivine and therefore also in the altered mineral.

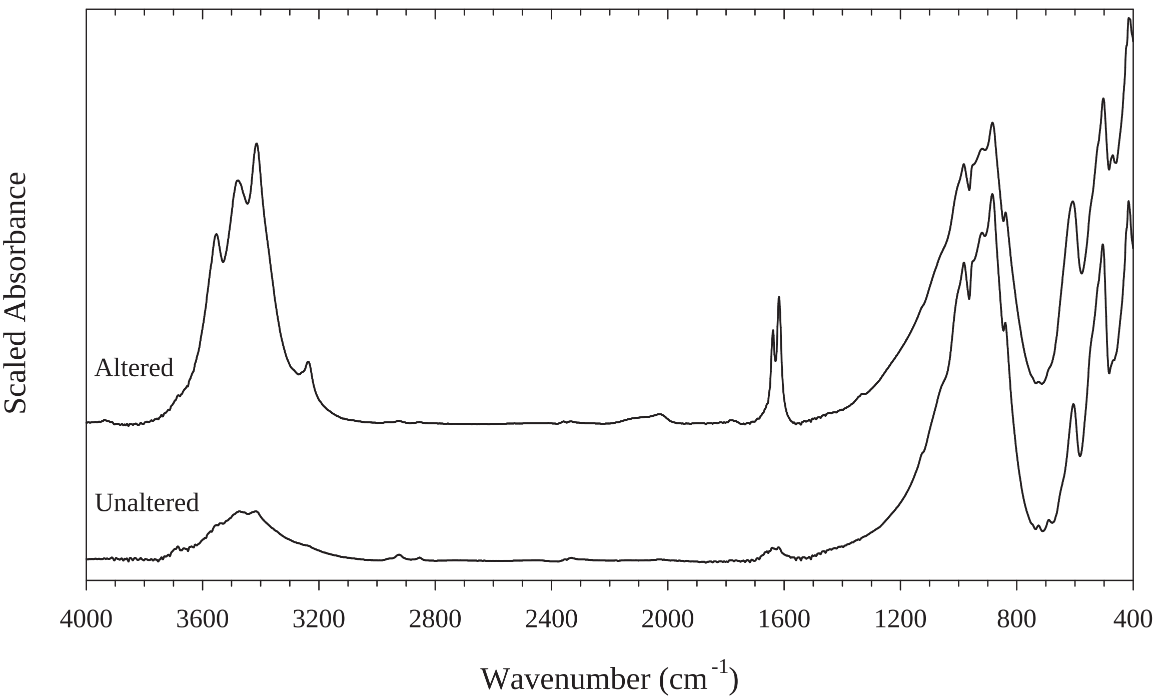

Fig. 18.—Mid-IR spectrum of the altered mineral in the cup from experiment S22 (top), compared with that of the unaltered mineral olivine (bottom).

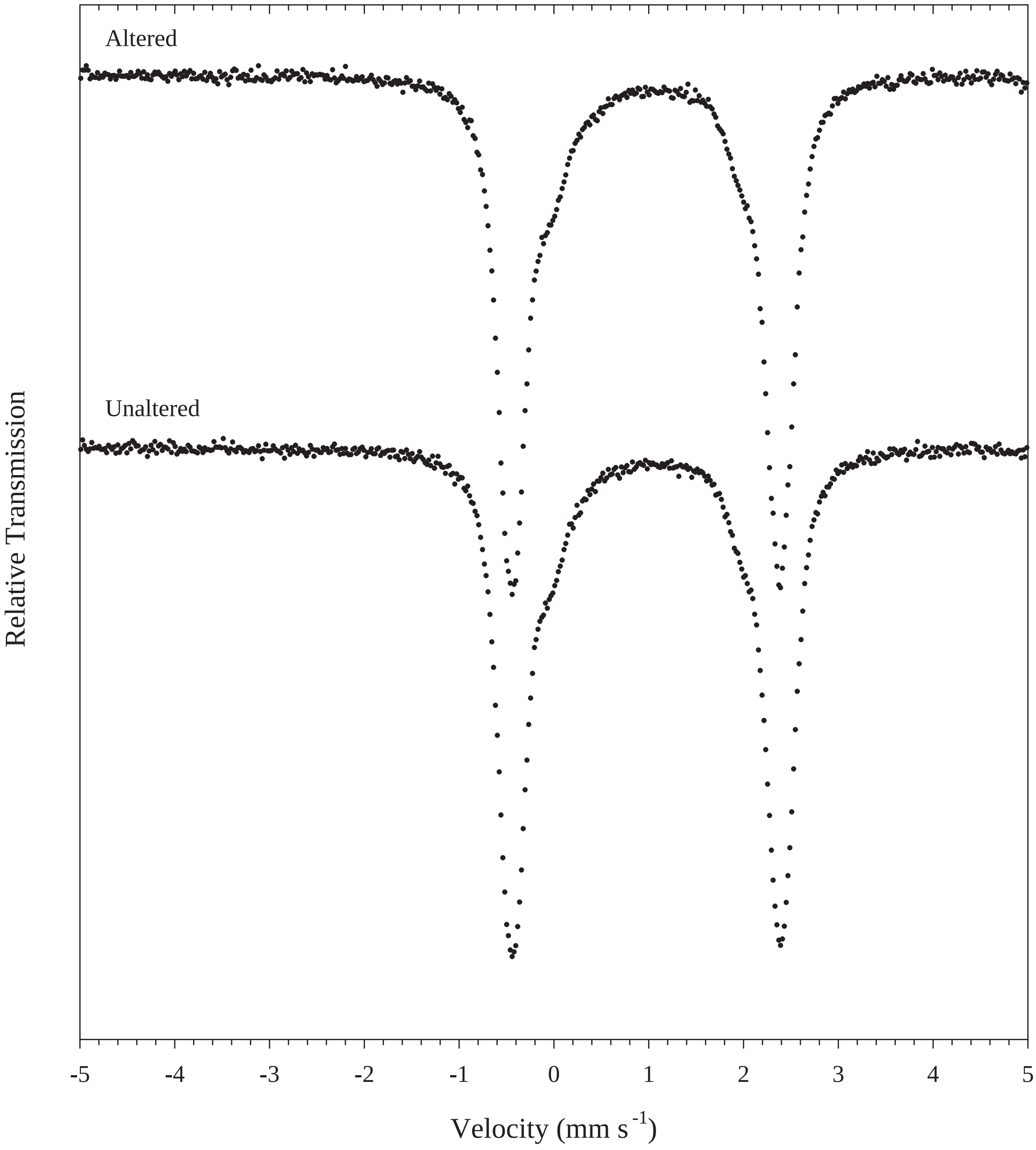

Fig. 19.—Mössbauer spectrum of the altered mineral in the cup from experiment S22 (top), compared with that of the unaltered mineral olivine (bottom).

4. DISCUSSION

4.1 Comparison of Products with Meteoritic Organics

The time evolution series of experiments (see Table 1) produced two important materials: one that was water soluble (Section 3.4) and one that was water insoluble (Section 3.5). The soluble material was dominated by ammonium carbonate but contained a very small amount of urea. The insoluble material was partly organic and partly mineral in character. The organic fraction is probably an aromatic nitrogen heterocycle with a high degree of ring symmetry. The aromatic ring is probably highly hydrogenated and substituted with amine groups, hydroxyl groups, or both. It was not possible to determine whether this orgainic material is free or bound into a macromolecule. The mineral fraction was mostly siderite with a small amount of ferric iron, probably in the form of Fe_2O_3.

Of the soluble materials, only urea has been detected in meteorites. Hayatsu et al. (1975) found urea with a concentration of 25 ppm in Murchison after extraction, where it seemed to be associated with the meteoritic organic macromolecular material. The urea produced in our experiments was probably produced by the dehydration of ammonium carbonate (see Section 3.4). The production of urea was very slow, as seen by the very small amounts recovered (less than 0.1 mg).

The detection of neither ammonium carbonate nor ammonium bicarbonate in meteorites has been reported in the literature, although it seems likely that these salts would have been present in the meteorite parent bodies. The minerals in the chondrite parent bodies were likely altered by water that contained CO_2 (Zolensky & McSween, 1988; Armstrong et al., 1982). If NH_3 was also present, it would have reacted quickly with such an aqueous fluid to form ammonium bicarbonate or ammonium carbonate, depending on the relative concentrations of CO_2 and NH_3. It is unlikely that NH_3 was abundant relative to N_2 in the Solar nebula but, if any were present, it would have condensed with H_2O and CO_2 in the form of ammonium bicarbonate and its concentration in icy planetesimals could have been much greater than its equilibrium value in the nebula (Lewis & Prinn, 1980). If ammonium carbonate were present in meteorite parent bodies, then it follows that it should have produced a small amount of urea by dehydration.

The association of urea with the meteoritic organic macromolecular material (Hayatsu et al., 1975) suggests that (a) either it was locked in this material and released after the acid treatment partly broke up the macromolecule, or (b) it was not present in the meteorite and only produced as a result of the acid treatment. Possibility (a) would imply that the meteoritic organic macromolecule formed during an aqueous alteration event in the parent body and trapped the urea. This assumes that the urea also formed during the same aqueous alteration event; however, it does not rule out the possibility that the meteoritic organic macromolecule and the urea were formed prior to their accretion into the parent body. Possibility (b) suggests that ammonium bicarbonate and ammonium carbonate were not sufficiently abundant to yield detectible amounts of urea, or that the urea so produced was consumed as it reacted with other species. In short, production of urea by the dehydration of aqueous ammonium carbonate is consistent with the presence of urea in meteorites, but it is not required by it.

The insoluble material is more problematic. Siderite, ferric iron, and nitrogen heterocycles are all present in carbonaceous chondrites, but they are only minor constituents. The major mineral phases of carbonaceous chondrite matrices are olivine and phyllosilicates (Buseck & Hua, 1993) and the major organic phase is the macromolecule (Cronin et al., 1988). The organic material produced in our experiments were associated with the siderite, but the organic compounds in carbonaceous chondrites are associated with fine grained phyllosilicate minerals (Pearson et al., 2002; Vali et al., 1998), not the carbonates.

The production of siderite in our experiments was determined to be the result of the action of aqueous CO_2 on the iron in the T316 stainless steel vessel. The intimate association of the siderite with the organic fraction of the isoluble material merits special attention. The siderite and organic material were not merely found as components of a casual mixture; rather, they appeared to be bound together into one homogeneous material. Also, when PAH was not added to the reactor (in experiment S23), the siderite was found only *beneath* the sample cup, in the vessel. Only when PAH was included did the siderite also form in the sample cup. The presence of heterocyclic nitrogen in the organic material may explain this observation. The electron pair of nitrogen would loosely bind aqueous iron. Once bound, the iron may bind aqueous carbonate and precipitate out of solution, taking the heterocycle with it. Iron from the vessel or lid must have dissolved in the aqueous solution and migrated inside the sample cup where it interacted with the organic material, formed carbonate, and precipitated. Apparently, without the heterocycle, the chemical properties of the aqueous solution prevented siderite from precipitating directly. The siderite in the vessel probably formed by aqueous carbonate binding directly to iron in the vessel, without the iron first dissolving in the fluid. This supported by the observation that the siderite at the bottom of the vessel was loosely bound to the metal, and had to be gently scraped free in order to collect it.

Significantly, experiment S22, where olivine was added, did not produce any siderite (see Sectiom 3.5). The olivine itself appears to have been altered somewhat, judging by the change in color, but its mid-IR and Mössbauer spectra show that it is still olivine. It should be noted that, if only the forsteritic component of the olivine were altered, its Mössbauer spectrum would not detect it. Such an alteration should have been visible in the mid-IR spectrum, but no significant change, other than the absorption of water by the olivine, was seen. In meteorites, primeval olivine underwent serpentinization, yielding the observed phyllosilicates (Zolensky & McSween, 1988).

The organic fraction of the insoluble material prodeced is different from the kind of nitrogen heterocycles detected in carbonaceous chondrites. The meteoritic nitrogen heterocycles in Murchison, Murray, and Orgueil include the purines adenine, guanine, hypoxanthine, and xanthine (Stoks & Schwartz, 1981), as well as the pyrimidine uracil (Stoks & Schwartz, 1979). These differ significantly in molecular structure from the nitrogen heterocycle proposed for the organic fraction of the insoluble material that we produced. The meteoritic organic macromolecular material seems to be composed of aromatic ring systems that contain heterocyclic nitrogen, oxygen, and sulfur, are hydrogenated, and are extensively cross-linked by short aliphatic chains (Cronin et al., 1988). This is also different from the organic material produced in our experiments, because it is highly symmetric, whereas the meteoritic organic macromolecular material is extremely heterogeneous.

4.2 Conclusions

It has been shown that PAH is reactive under the conditions employed in our reactor; however, the products we observed are not representative of the major constituents in meteorites. Ammonim carbonate, ammonium bicarbonate, and urea have been identified as soluble products (see Section 3.4). To our knowledge, there has been only one report of the detection of urea in meteorites (Hayatsu et al., 1975). This may be due to the fact that much of the analysis of free meteoritic organics has been focused on the more biologically significant molecules, such as amino acids and carboxylic acids. A search for ammonium carbonate and ammonium bicarbonate seems to have been largely overlooked in the literature, especially in the context of the origins of the meteoritic organic matter.

The water-insoluble organic product was probably a highly symmetric aromatic nitrogen heterocycle that is hyrdogenated and highly substituted (see Section 3.5). This kind of heterocycle has not been detected in meteorites. Regardless of its occurrence in meteorites, PAH does transform under the conditions in our experiments. These conditions are qualitatively representitive of those expected in meteorite parent bodies, but they are rather exaggerated. Also, the PAH we used in the vast majority of these experiments, pyrene, is not quite representitive of the expected organic materials that accreted into the parent bodies. The primary source of organic carbon that accreted into the meteorite parent bodies may have been the organic refractory material in the interstellar medium (Sephton & Gilmour, 2000). This material is similar to the meteoritic macromolecule, but the aromatic ring systems in the interstellar material are expected to be much larger than those in meteorites. The PAH used in our experiments was meant to represent the free aromatic molecules found in meteorites, which may have resulted from aqueous alteration of the meteoritic macromolecule. Our experiments suggest that these free aromatics may have also been altered during a similar aqueous alteration event in the meteorite parent body.

4.3 Estimated Errors in Gas Quantities

The solubility of NH_3 in water at 25°C and 1 bar is 31% (Stecher, 1968). Due to this extremely high solubility, the molar quantity of this gas may be grossly underestimated in our experiments. For example, if the absorption of NH_3 in water were instantaneous, we may suppose that the water would become saturated while charging the reactor. This would require 86 mmol of NH_3. This absorption is not instantaneous because the pressure in the reactor was observed to decrease rapidly from 1 to 0 bar after charging the reactor with NH_3, but this may certainly serve as an upper bound. On the other hand, if the absorption were so slow as to be negligible, then the 20 ml of head space would hold 0.81 mmol of NH_3. Again, this is not the case, but does serve to establish a lower bound. Either case would yield a final equilibrium pressure of approximately 1 bar in the reactor (the vapor pressure of water under these conditions), so the amount of NH_3 delivered to the reactor may reasonably be anywhere between 0.81 mmol and 86 mmol, representing a possible range of error spanning two orders of magnitude.

CO_2 is less soluble in water than NH_3. The solubility of CO_2 in water at 25°C and 1 bar is 0.0614 mol% (Lide, 1993). At 25°C and 25 bar the solubility rises to about 1.625 mol% (Diamond & Akinfiev, 2003). If we use the same criteria as for NH_3 to establish upper and lower bounds for CO_2, while noting that the final pressure is now 25 bar, then the lower bound, set by 25 bar of gas in the 20 ml of head space, is 20.2 mmol. The upper bound, set by the *additional* complete solvation of CO_2 in the 5 ml water, is 24.7 mmol.

The error here is more reasonable; however the possible range of error is still significant. More seriously, it is not the solubility of CO_2 in pure water that is relevant here, but the solubility of CO_2 in water containing a variable amount of dissolved NH_3. The greatly increased solubility of CO_2 in this basic solution is exacerbated by an immediate reaction producing ammonium carbonate and ammonium bicarbonate. This suggests establishing a new upper bound for CO_2 set by the immediate and complete reaction with the dissolved NH_3 to form ammonium bicarbonate, beyond the upper bound determined from the assumption of a pure water solution. Note that initially the addition of CO_2 will yield ammonium carbonate, but, since the reaction is assumed to be instantaneous, and the amount of CO_2 is initially unlimited, the reaction will shift in favor of ammonium bicarbonate as the molar ratio of CO_2 to NH_3 passes 0.5 and continues past 1. Once this molar ratio reaches unity, all of the NH_3 will be bound in ammonium bicarbonate. The upper bound of 86 mmol NH_3 will bind 86 mmol CO_2; however, this reaction will also consume 1 mol H_2O for every mole of NH_3. The upper bound of NH_3 would therefore reduce the volume of water from 5 ml to 3.5 ml. As CO_2 continues to enter the reactor, it will dissolve in this volume of water, and then pressurize the 20 ml of head space. The upper bound for CO_2 delivered to the reactor then becomes 109 mmol.

The assumptions leading to these upper and lower bounds are extremely naïve. NH_3 absorption in water appears to be swift, but not instantaneous. CO_2 absorption in ammonia water is probably not so high that it completely binds all of the NH_3, and the solubility of CO_2 in the resulting solution would not be similar to that in pure water. The upper bounds represent the worst-case error. The primary source of error is in the amount of NH_3 delivered to the reactor. If this can be better constrained, then the uncertainty in the amount of CO_2 will also be better constrained. With the assumpition that all of the NH_3 dissolved in the water reacts with CO_2 to form an ammonium salt, the amount of NH_3 can be roughly estimated from the amount of ammonium salt found in the reactor at the end of each experiment.

4.4 Future Work

Possibly the biggest problem with the current experimental arrangement is the head space in the reactor. There is currently about 25 ml of head space versus 5 ml of reaction volume (5 ml water). This only accounts for the volume of the Teflon insert, and not the valves and internal passages and extrusions of the head. Also, the reactor is heated from the sides and bottom of the vessel. The head is somewhat cooler. PAH has been observed to condense on the interior of the lid and in the valves, whereas all alteration products were found in, under, and around the water in the sample cup. This results in poor yield. Only one experiment was performed with a mineral counterpart (olivine) to the organic constituent (pyrene), and in this experiment these two materials were not intimately mixed. The olivine mostly sank, and the pyrene mostly floated.

To overcome problems of head space and temperature differentials, a small T316 stainless steel insert with Swagelok end caps could be used (see Sephton et al., 1998). This could effectively reduce the volume to about 1 ml. The standard experiment should include PAH, CO_2, NH_3, H_2O, and a mineral in this sealed insert. The materials should be well mixed. The sealed insert could then be placed in the current reactor with enough water to cover the insert. The remaining head space of the reactor could be purged with N_2 to prevent oxidation. The water would ensure good thermal contact between insert and reactor vessel, and could be used to minimize pressure differentials across the vessel walls. Alternatively, the "inserts" may simply be placed in an oven if they can remain sealed and intact at the anticipated internal pressure. Unfortunately, this design will not allow the direct measurement of internal pressure. The experiment should run at about 100°C for at least 5 days, but 20 days or longer may be better because yields may be higher. Different temperatures could be tried. Several experiments could be run simultaneously in different inserts.

The loading of the insert may pose a small technical challenge. It must be loaded at atmospheric pressure, but it must be operated at higher pressure (possibly much higher than the increase in pressure expected at running temperature). The use of Swagelok end caps would also preclude the use of a mixing line to add gases. However, all materials may be loaded easily as solids. Dry ice could be used for CO_2. Alternately, it could be dissolved in H_2O first and then frozen. This would limit the amount of CO_2 added to the amount soluble in the given volume of H_2O. NH_3 is much more soluble in H_2O than CO_2. Dissolving a set amount of NH_3 in H_2O and then freezing may be the best way to add NH_3. The CO_2 should be added separately as a solid if NH_3 is added dissolved in the H_2O to prevent premature reaction of the materials. The reaction between CO_2 with NH_3 in H_2O is fast and may increase the uncertanty in the amount of CO_2 added. The H_2O should be de-gassed prior to the addition of NH_3, for example by sonification. These frozen solids should be powdered and then mixed together with the mineral and PAH. Keeping everything frozen during loading may pose a problem. Extra head space may be needed to prevent over-pressurizing the insert due to the increase in volume of the liquid H_2O at the temperature of the experiment. It would be best to evacuate the extra head space, but filling it with an inert gas like N_2 should suffice.

Unloading the reactor may also be a problem. The pressure inside may be reduced by placing the insert in ice or perhaps liquid N_2 before opening. The samples should be analyzed by gas chromatography-mass spectrometry. Retaining gases when the unloaded samples return to room temperature and pressure may be a problem if they are to be analyzed, whereas the liquid could be loaded to the gas chromatograph by direct injection, using a syringe. Other materials may be extracted from the solids by standard meteorite analysis techniques in the literature. Other solids should be analyzed by mid-IR spectroscopy. The mineral may be studied by Mössbauer spectroscopy, or perhaps X-ray diffraction or transmission electron microscopy if possible.

Different experiments could be performed by varying the initial PAH (or perhaps by using a different organic precursor), the initial mineral (e.g. olivine vs. a pyroxene such as enstatite), the temperature, the expected pressure (perhaps by varying the amound of head space), the relative amounts of CO_2, NH_3, and H_2O, and the running time. As an alternate to adding frozen CO_2 and ammonia water, ammonium carbonate may be added instead of or in addition to them. This may help test the effect of of the initial source of these materials on the resulting product, which may help constrain the organization of the precursors during parent body accretion.

LIST OF REFERENCES

Allamandola, L. J., Tielens, A. G. G. M., & Barker, J. R. 1985, ApJ, 290, L25

Anders, E., & Grevesse, N. 1989, Geochim. Cosmochim. Acta, 53, 197

Armstrong, J. T., Meeker, G. P., Huneke, J. C., & Wasserburg, G. J. 1982, Geochim. Cosmochim. Acta, 46, 575

Burnett, D. S., Woolum, D. S., Benjamin, T. M., Rogers, P. S. Z., Duffy, C. J., & Maggiore, C. 1989, Geochim. Cosmochim. Acta, 53, 471

Buseck, P. R., & Hua, X. 1993, Annual Review of Earth and Planetary Sciences, 21, 255

Coblentz Society, Inc. 2005, in NIST Chemistry WebBook, NIST Standard Reference Database Number 69 (Gaithersburg: National Institute of Standards and Technology), http://webbook.nist.gov

Cooper, G., Kimmich, N., Belisle, W., Sarinana, J., Brabham, K., & Garrel, L. 2001, Nature, 414, 879

Cronin, J. R., & Moore, C. B. 1971, Science, 172, 1327

Cronin, J. R., Pizzarello, S., & Cruikshank, D. P. 1988, in Meteorites and the Early Solar System, ed. J. F. Kerridge & M. S. Mathews (Tucson: Univ. Arizona Press), 819

Diamond, L. W., & Akinfiev, N. N. 2003, Fluid Phase Equilibria, 208, 265

Grimm, R. E., & McSween, H. Y. 1989, Icarus, 82, 244

Hartmann, W. K. 1993, Moons & Planets, 3rd edn. (Belmont: Wadsworth)

Hayatsu, R., Anders, E., Studier, M. H., & Moore, L. P. 1975, Geochim. Cosmochim. Acta, 39, 471

Hayatsu, R., Matsuoka, S., Anders, E., Scott, R. G., & Studier, M. H. 1977, Geochim. Cosmochim. Acta, 41, 1325

Junk, T., & Catallo, J. W. 1996, Tetrahedron Letters, 37, 3445

Katritzky, A. R., Daniel, A. N., Siskin, M., & Balasubramanian, M. 2001, Chem. Rev., 101, 837

Kerridge, J. F., Chang, S., & Shipp, R. 1987, Geochim. Cosmochim. Acta, 51, 2527

Keuleers, R., Desseyn, H. O., Rousseau, B., & Van Alsenoy, C. 1999, J. Phys. Chem. A, 103, 4621

Lewis, J. S., & Prinn, R. G. 1980, ApJ, 238, 357

Lide, D. L., ed. 1993, CRC Handbook of Chemistry and Physics, 74th edn. (Boca Raton: CRC Press)

McCollom, T. M., Simoneit, B. R. T., & Shock, E. L. 1999, Energy and Fuels, 13, 401

Pearson, V. K., Sephton, M. A., Kearsley, A. T., Bland, P. A., Franchi, I. A., & Gilmour, I. 2002, Meteoritics and Planetary Science, 37, 1829

Penzias, A. A. 1980, Science, 208, 663

Sears, D. W. 1978, The Nature and Origin of Meteorites, Monographs on Astronomical Subjects No. 5 (New York: Oxford University Press)

Sephton, M. A., & Gilmour, I. 2000, ApJ, 540, 588

Sephton, M. A., Pillinger, C. T., & Gilmour, I. 1998, Planet. Space Sci., 47, 181

Shock, E. L., & Schulte, M. D. 1990, Nature, 343, 728

Stecher, P. G., ed. 1968, The Merck Index, 8th edn. (Rahway: Merck & Co., Inc.)

Stoks, P. G., & Schwartz, A. W. 1979, Nature, 282, 709

—. 1981, Geochim. Cosmochim. Acta, 45, 563

Vali, H., Golden, D. C., Sears, S. K., Ciftcioglu, N., Williams-Jones, A. E., McKay, D. S., Thomas-Keprta, K. A., Ming, D. W., & Zolensky, M. E. 1998, in Lunar and Planetary Institute Conference Abstracts, 1835

Wade, M. L., Agresti, D. G., Wdowiak, T. J., Armendarez, L. P., & Farmer, J. D. 1999, J. Geophys. Res., 104, 8489

Wannier, P. G. 1980, ARA&A, 18, 399

Wasson, J. T. 1974, Meteorites: Classification and Properties (Berlin and New York: Springer-Verlag)

Wdowiak, T. J., & Agresti, D. G. 1984, Nature, 311, 140

Wilson, L., Keil, K., Browning, L. B., Krot, A. N., & Bourcier, W. 1999, Meteoritics and Planetary Science, 34, 541

Yang, J., & Epstein, S. 1983, Geochim. Cosmochim. Acta, 47, 2199

Zolensky, M., & McSween, H. Y. 1988, in Meteorites and the Early Solar System (Tucson: Univ. Arizona Press), 114